

MULTITEMPORAL LAND COVER CLASSIFICATION OF
THE LITTLE WASHITA WATERSHED USING
THE KAUTH-THOMAS GREENNESS
VEGETATION INDEX

By

CHRISTOPHER G. BERRY

Bachelor of Arts

University of Northern Colorado

Greeley, Colorado

1992

Submitted to the Faculty of the
Graduate College of the
Oklahoma State University
in partial fulfillment of
the requirements for
the Degree of
MASTER OF SCIENCE
May, 1998

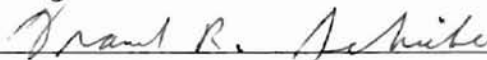
MULTITEMPORAL LAND COVER CLASSIFICATION OF
THE LITTLE WASHITA WATERSHED USING
THE KAUTH-THOMAS GREENNESS
VEGETATION INDEX

Thesis Approved:



Thesis Advisor







Dean of the Graduate College

ACKNOWLEDGEMENTS

I wish to express my sincere appreciation to my major advisor, Dr. David Waits, for his encouragement, guidance, assistance, and friendship. My appreciation extends to my other committee members Dr. Frank Schiebe and Dr. Stephen Stadler. The opportunity, support, and financial assistance provided by Dr. Frank Schiebe and the National Agricultural Water Quality Laboratory were invaluable to my research. I would like to thank Dr. David Waits, Dr. Stephen Stadler, and the Department of Geography for providing me with the opportunity to conduct this research as well as their financial support.

I also wish to express my deep gratitude to those who provided suggestions, assistance, and friendship in my efforts: John Anderson, Daniel Umbach, Joseph Seig, and Daniel Yuen. Special thanks go to my good friends Shannon Morrissey, Andrew and Christie Plackner, Duncan Maeer, Mike Owens, Lisa Brown, David Goughnour, Eric Christian, Owen Rock, and Gina Bloodworth for making these years most enjoyable.

I would like to thank everyone in the Department of Geography for their help, especially Susan Shaul and Kimberly Cundiff, whose efforts are greatly appreciated.

I also want to thank my love, Amy Weeks, for constant encouragement through everything.

Finally, my deepest thanks go to my parents, Jack and Maribeth Berry, for their unending support, guidance, and encouragement throughout my life.

TABLE OF CONTENTS

Chapter	Page
I. INTRODUCTION.....	1
Background and Problem Statement.....	1
Purpose of the Study	4
Study Area	5
Objectives	7
Multispectral Imagery Sources	8
Scope and Limitations	11
II. LITERATURE REVIEW.....	14
Radiometric Correction for Multitemporal MSS Imagery.....	14
Multispectral Dimension Reduction.....	17
Studies Involving Multitemporal Land Cover Dynamics.....	21
Accuracy in the Registration of Overlaid Images.....	27
III. METHODOLOGY.....	29
Chapter Overview.....	29
Image Loading and Subsetting.....	31
Radiometric Correction.....	32
Geometric Correction.....	35
Derivation of the Greenness Vegetation Index.....	37
GVI Composite Construction and Interpretation.....	38
Unsupervised Classification of the GVI Composite Image.....	40
IV. ANALYSIS AND RESULTS.....	43
Methodology of Analysis.....	43
Multitemporal Land Cover Class Spectral Signatures.....	45
Classification Results for Each Year.....	55
V. CONCLUSIONS.....	65
Summary.....	65
Discussion of Research Findings.....	66
Recommendations for Future Research.....	67
BIBLIOGRAPHY.....	69

LIST OF TABLES

Table	Page
I. MSS Scene Dates and Status For Years Used To Develop Multitemporal Classification Procedure	12
II. Landsat MSS Spectral Bands.....	33
III. Landsat MSS Post-Calibration Dynamic Ranges for U.S. Processed Data.....	34
IV. Landsat MSS Solar Spectral Irradiance Values.....	34
V. Cluster Spectral Signature Listing for 1976.....	46
VI. Cluster Spectral Signature Listing for 1984.....	47
VII. Cluster Spectral Signature Listing for 1986.....	48
VIII. Cluster Spectral Signature Listing for 1988.....	49
IX. Average Spectral Signatures for 1976.....	51
X. Average Spectral Signatures for 1984.....	52
XI. Average Spectral Signatures for 1986.....	53
XII. Average Spectral Signatures for 1988.....	54
XIII. Combined Average Spectral Signature Statistics.....	55
XIV. Class Pixel Counts for 1976.....	61
XV. Class Pixel Counts for 1984.....	61
XVI. Class Pixel Counts for 1986.....	62
XVII. Class Pixel Counts for 1988.....	62
XVIII. Acres in Selected Class Groups.....	63

LIST OF FIGURES

Figure	Page
1. Map of the Little Washita Watershed.....	6
2. Typical Spectral Reflectance Curves for Vegetation, Soil, and Water.....	9
3. Radiometric Response Function.....	16
4. The Tasseled Cap.....	19
5. False-Color Composite of 3 GVIs -May, June, & November, 1988.....	39
6. Multitemporal Land Cover Classification for 1976.....	56
7. Multitemporal Land Cover Classification for 1984.....	57
8. Multitemporal Land Cover Classification for 1986.....	58
9. Multitemporal Land Cover Classification for 1988.....	59

CHAPTER ONE

INTRODUCTION

Background and Problem Statement

Remote sensing has become an important source of land cover information for practical geographic applications. Classifications derived from multispectral satellite imagery can be useful tools for determining land cover for monitoring environmental concerns and natural resource inventory. Detecting change in land cover over time is especially valuable for applications which investigate and implement policy regarding land use. Land use/land cover information is used for the location and measurement of non-point sources in water pollution models (Fostel et al., 1979). Variations in land cover affect physical characteristics of the land such as albedo, emissivity, roughness, and plant transpiration which in turn influence the hydrological cycle and land-atmosphere energy fluxes (Lambin and Strahler, 1994). Land use/land cover classifications are, therefore, essential for input in hydrologic models. This study will investigate the development of a procedure for the derivation of multitemporal land cover information from multispectral satellite data. The land cover classifications produced by this study will be used for hydrologic modeling in a larger project involving the Little Washita Watershed in southwestern Oklahoma.

Most land cover classifications are generated from single image data sets acquired at one instant in time, so assessing land cover changes at various times during a year

using conventional approaches requires multiple images and classifications. A multitemporal approach is preferred because classifications derived from a single-date image rarely contain enough information to spectrally distinguish different cover types, or to adequately represent all land cover types present in an area over a period of time (Lo et al., 1986).

During a growing season, land cover will change, and it will also change from year to year. For example, a classification derived from an image of Oklahoma acquired in the spring will contain areas where winter wheat was growing. An image depicting the same area in the summer will show no winter wheat and will also contain indications of crops such as corn or grain sorghum that were not being grown in the spring. A classification derived from the spring image would represent only those agricultural classes present at that time, but any other classes for crops planted later in the growing season would be absent.

When conducting multiple-year studies, numerous classifications which may be composed of differing land cover classes can become difficult to compare. Every satellite scene requires extensive image processing and classification procedures that sometimes produce results that do not conform with other classifications. Images acquired at different dates represent various types of land cover in different states of growth and result in different spectral signatures for the same cover type. Different planting dates for any crop result in growth states that are dissimilar both in one growing season and from year to year. For this reason, different crops may have identical spectral signatures in one image, or in the comparison of two scenes from different years. A spectral signature is the distinctive reflectance and emittance properties of a particular land cover type, which

will usually exhibit a pattern that differs from other types (Avery and Berlin, 1992).

Single-date classifications derived from a set of images acquired at different dates usually consist of a set of land cover classes which do not reflect the temporal nature of the data (Singh, 1989). Such classifications may have only a single class to represent agricultural crops if no field verification data is available to identify different crop types and derive their individual spectral signatures.

These problems give rise to a need for improved methods of using multispectral data for land cover change detection. A single image which can display changes in land cover through one growing season based on temporal data would be more effective for some purposes than several single-date classifications. Such an image could be classified according to multitemporal land cover classes that are appropriate for the growth stages present during a growing season. These classes would represent all types of cover present in every image and identify at which points in time those cover types existed, depending on the number of scenes used and the dates of acquisition. This approach would allow for the identification of different types of crops based on the growth patterns of the vegetation in an area throughout a growing season. The process would require normalization of the solar illumination differences inherent in images acquired at different times, and the registration of each image to real-world coordinates to ensure accuracy when overlaying images. Also required would be the reduction in the redundancy and dimensionality of the data, the combination of scenes from different dates into a single image, and a method of classifying that image using land cover classes that are appropriate for the data set. Studies performed by Howarth and Boasson (1983)

and Lo et al. (1986), among others, used similar methods that will be described in the Literature Review chapter.

Purpose of the Study

The US Department of Agriculture (USDA) - Agricultural Research Service's National Agricultural Water Quality Laboratory (NAWQL) in Durant, Oklahoma selected the Little Washita Watershed in southwestern Oklahoma as its target for an ongoing experiment with the objective to "test the usefulness of remotely sensed data in hydrologic modeling" (Jackson and Schiebe, 1992). The NAWQL has collected a long time-series of hydrologic data using conventional ground sources and remotely sensed methods, focusing on soil moisture and evaporative change. Microwave radiometers, multispectral scanners, and imaging radar were flown aboard two NASA aircraft and used to obtain data in 1992. Land cover information focusing on crop cover inventory is needed for entry into the time-series hydrologic model for the purposes of the larger Little Washita project. The purpose of the research described in this thesis was to develop a procedure to derive land cover information from satellite data representing one growing season in order to create multitemporal land cover classifications for entry into the hydrologic model.

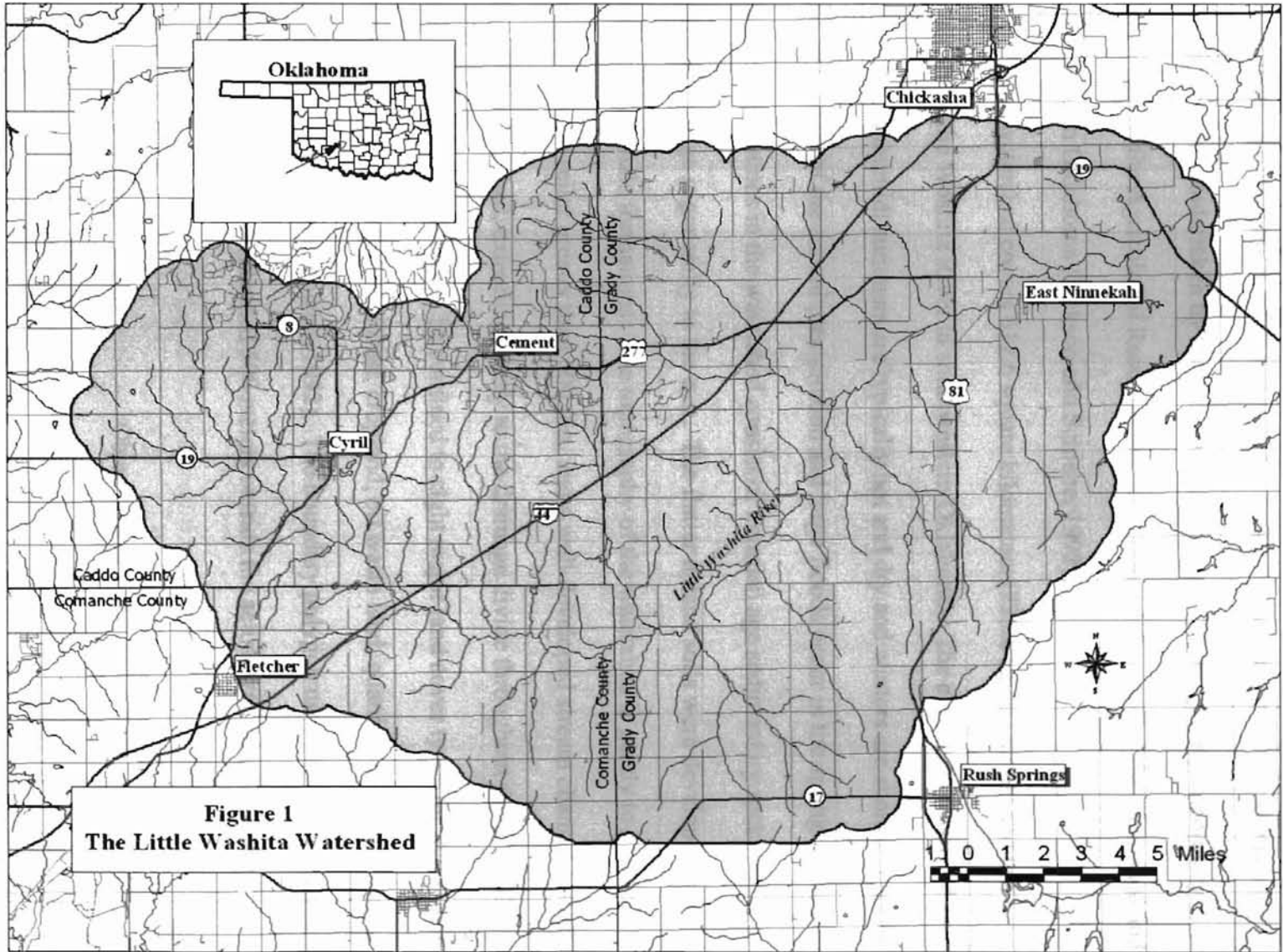
Satellite-based multispectral imagery has been collected and archived since the launch of Landsat 1 in 1972. That satellite and the four subsequent Landsat satellites carried the Multispectral Scanning System (MSS) radiometers. MSS scenes from every even-numbered year from 1972 to 1992 are to be used to create a database of

multitemporal land cover information for the watershed that will be used in the NAWQL's hydrology project. This set of MSS imagery was used to develop the procedure for creating that database. Thematic Mapper (TM) and SPOT imagery was also used for more recent land cover analyses and will be used in future work on the project, as the MSS sensors are no longer used to collect data.

Large amounts of hydrologic and meteorologic data have been collected from the Little Washita Watershed, which makes the area extremely useful for study with remotely sensed imagery (Allen and Naney, 1991). The multitemporal land cover classification method described in this study represents an attempt to research the potential of satellite imagery in collecting data for use in monitoring human activity and impact in the Little Washita watershed.

Study Area

The area of this study was the Little Washita River Watershed, which has been the target of extensive research since the late 1930s when the area was chosen for a national project for soil erosion control. Since the 1940s, the USDA - Natural Resource Conservation Service (NRCS) has applied extensive soil and water conservation structures and measures. The USDA - Agricultural Research Service (ARS) began collecting hydrologic data on the watershed in 1961. An extensive rain gauge network and stream gauges have been used to measure continuous flow, suspended sediment transport, and water quality. The area was one of seven watersheds nationwide that were chosen in 1978 for the Model Implementation Project, which was to demonstrate the



effects of intensive land conservation treatments on water quality in watersheds that are larger than 25 square miles. The watershed is presently the subject of an extensive hydrology study undertaken by the National Agricultural Water Quality Laboratory (NAWQL) of the Agricultural Research Service. Figure 1 is a map of the watershed and its location in Oklahoma (Jackson and Schiebe, 1992).

The watershed covers 612.6 square kilometers (235.6 square miles) and is a tributary of the Washita River in southwestern Oklahoma. The climate is classified as moist and subhumid; summers are typically hot and dry and winters are short, temperate and dry. Most of the annual precipitation and large floods occur in the spring and fall. Bedrock formations in the watershed consist of Permian age sedimentary rocks and surface drainage is generally to the east. The flatter upland soils were developed from fine-textured shale formations. The topography of the watershed is gently to moderately rolling with no relief greater than 600 feet, and a well-developed stream channel system drains the watershed, extending nearly to the drainage divide throughout the area. The land use in the watershed can be confined to eight major land cover types for hydrologic purposes: rangeland, pasture, forest, cropland, oil waste land, quarries, urban/highways, and water (Jackson and Schiebe, 1992). The boundary polygon used for this study and shown in Figure 1 was extended 500 meters outside the actual watershed boundary.

Objectives

The main objective of this study was to develop a procedure to define, create, and evaluate a multitemporal land cover classification which indicates cover changes through

a growing season using multispectral imagery. This process was developed to address the problems, as described earlier, which are associated with the comparison of single-date classifications derived from imagery for which no field verification information is available. The further objective of this research is to use this procedure to create a land cover database from Landsat MSS data for every even-numbered year from 1972 to 1992 for the Little Washita project, and to continue deriving land cover information in the future from Landsat Thematic Mapper and SPOT imagery. However, due to limitations in the data which will be explained in the Scope and Limitations section, only four of these years could be used effectively for this study. The satellite platforms and their sensors will be described in the Multispectral Imagery Sources section below.

Multispectral Imagery Sources

The imagery used in this study was that acquired by Landsat MSS. This sensor was first launched on the ERTS-1 satellite in July of 1972, and was included on the four subsequent Landsat satellites. Other multispectral satellite imaging systems such as Thematic Mapper (1982) and SPOT (1986) have since been launched which have also been used to provide some ancillary data for this study, and will be used in future land cover classifications for the Little Washita project. However, only MSS imagery was used for the development of the classification procedure in this study, in order to provide a spatially and spectrally consistent data set. The MSS sensors aboard Landsats 4 and 5 are no longer used to collect data, so the methods developed in this study were designed

to be applicable to other imagery sources for future research. The following discussion is a short comparison of each scanning system.

The MSS collects data in four wavelength bands, with two bands which sense visible light and two which sense near-infrared energy. Bands 1 and 2 record green (0.5 to 0.6 μm) and red (0.6 to 0.7 μm) light, respectively. Comparisons between these and the near-infrared bands, band 3 (0.7 to 0.8 μm) and band 4 (0.8 to 1.1 μm), are useful for the detection of vegetation (Avery and Berlin, 1992). Figure 2 shows that in the near-

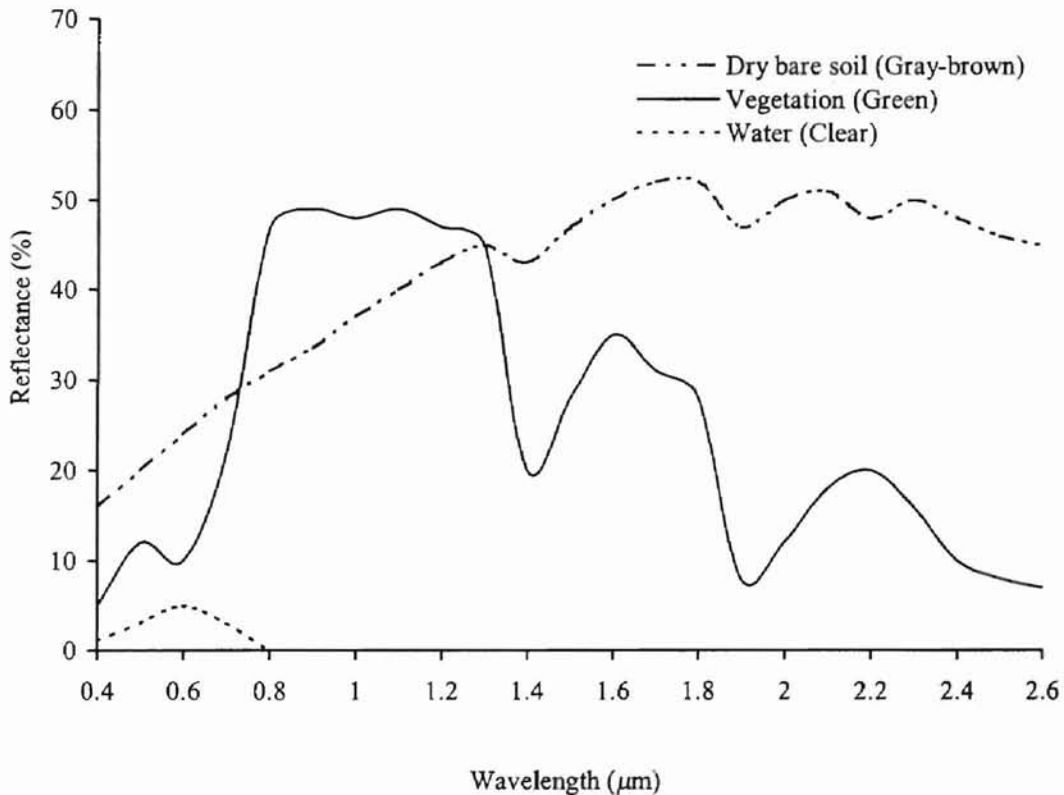


Figure 2. Typical spectral reflectance curves for vegetation, soil, and water (Lillesand and Kiefer, 1992).

infrared region of the electromagnetic spectrum plant reflectance is typically 40 to 50 percent of the incident energy, but is much lower in the visible portion. Comparisons between bands result in distinct spectral response patterns, or spectral signatures for

different land covers such as vegetation, soil, and water. Landsat Thematic Mapper (TM) imagery uses three more bands than MSS, allowing for more information and therefore better means of distinguishing land cover types. TM scanners use three visible bands, one near-infrared, two mid-infrared, and one thermal band. The visible and near-infrared band-widths are narrower than those of MSS and are centered on areas of maximum sensitivity to plant vigor, which means they are more finely tuned for sensing vegetation. SPOT imagery uses only three bands, two visible and one near-infrared, which are also narrower than MSS bandwidths (Lillesand and Kiefer, 1992).

Radiometric resolution refers to the digital number range used when a multispectral scanner converts analog energy signals to digital format. MSS data is scaled between 0 and 127, except for band 4 on Landsats 1, 2, and 3, which is between 0 and 63. Both TM and SPOT use radiometric resolutions of 0 to 255. The increase in Digital Number (DN) scale enables these scanners to display a greater range of gray tones in each band, which reveals more information about the reflectivity being measured.

The spatial resolution of these three systems also affects the accuracy of land cover classification. The instantaneous field of view (IFOV) of a scanner is the ground area represented by one pixel in an image. MSS has an IFOV of about 80m x 80m, TM's is 28.5m x 28.5m, and the SPOT multispectral scanner's is 20m x 20m (Avery and Berlin, 1992). Increasing spatial resolution reduces the number of mixed pixels, which contain more than one land cover type, but also results in a larger number of pixels needed to view the same area of land, which increases the size of image files and processing time.

The improvements in the quality of raw data produced by TM and SPOT sensors have helped to increase accuracy in land cover analyses, but with increased costs as well. MSS imagery is available at a lower cost and, having been archived since 1972, represents a long time-series of data from which to extract information for the procedure development for this research. Also, the data transformations used in this study which will be described in the Literature Review chapter have been shown to increase the information potential of MSS images, and can be applied effectively to TM and SPOT imagery.

Scope and Limitations

Three MSS scenes from every even-numbered year from 1972 to 1992 were supplied by the NAWQL for this research. The three scenes for each year represented distinct and important points in a growing season. Spring images acquired before May displayed winter wheat that was planted the year before at its peak of growth in the Little Washita region. In summer scenes, those fields planted in wheat were harvested and had a bare soil or stubble ground cover whereas summer crops such as grain sorghum were at their peak greenness. Images acquired in the fall showed winter wheat that had been planted for harvest the next year and the senescence of summer crops. Examination of these three points in a growing season made it possible to identify different land covers based on these growth patterns. Woodlands showed vigorous growth in spring and summer but were nearly barren in the fall, depending on the date. Rangelands showed a

similar pattern, but had a lower infrared response than dense trees. Urban areas and water bodies, of course, had little or no vegetative cover.

The eleven-year set of MSS images was examined to determine the years that were suitable to create the classification procedure for this study. The overabundance of clouds in some scenes excluded those from being used. Minimal cloud cover (less than 10%) could be overlooked, but those scenes containing a higher percentage of ground obstruction, including cloud shadow, were unusable. Cloud presence not only covers and negates the data in a single image, but in this multitemporal application, creates additional false spectral signatures when combined with other cloud-free images from the same year. Unfortunately, scenes acquired in summer were rarely cloud-free. Four years

TABLE I
MSS SCENE DATES AND STATUS FOR YEARS USED
TO DEVELOP MULTITEMPORAL CLASSIFICATION PROCEDURE

YEAR	SCENE DATE	IMAGE QUALITY
1976	16 April	Good
	16 July	Cloudy - Not Used
	11 August	Good
	13 October	Good
1984	10 May	Good
	5 July	Good
	10 November	Good
1986	14 April	Good
	27 July	Good
	31 October	Good
1988	13 May	Good
	30 June	Good
	1 August	Cloudy - Not Used
	5 November	Good

were selected that were acceptable for this research. Table I is a list of the MSS scenes and their quality for the years that were used in this study.

The absence of field verification information, or ground truth, for the imagery from the years that were used also presented limitations in the classification of the data. A knowledge of the ground cover present at the time of acquisition is needed to determine the accuracy of a land cover classification. However, using some ancillary data such as aerial photos, topographic maps, and “windshield surveys,” conclusions were drawn about ground cover using image interpretation techniques such as field shape and size, texture, feature association, and recognition. The process used to determine land cover information for the years used in this study will be explained in the Analysis and Results chapter.

This thesis will illustrate that the classifications derived from these years represent the development of a valid method of land cover change detection using multitemporal satellite imagery. This procedure was applied to the historical MSS data supplied by the NAWQL for this study and will be used for future classifications of TM and SPOT imagery of the Little Washita Watershed.

CHAPTER TWO

LITERATURE REVIEW

Radiometric Correction for Multitemporal MSS Imagery

The use of satellite imagery and spectral indices to monitor land cover is extensive, but the normalization of the digital data in accordance to the calibration of the sensors is sometimes ignored (Price, 1987). The data set for the study consisted of images from five MSS units which acquired images using different sensor calibrations at different times with different solar illumination conditions, resulting in images whose Digital Number (DN) values could not be compared directly. To correct this problem, a radiometric correction was performed, normalizing each image's DN values in relation to all other MSS scenes. This operation converted the image's raw DN values into exoatmospheric reflectance; that is, a unitless value of the radiance reflected to the top of the earth's atmosphere, which is received by the satellite (Lillesand and Kiefer, 1994). This process removed the effect of sun elevation angle differences and the eccentricity of the earth's orbit (Schiebe et al., 1992). This process can also be used for the radiometric correction of raw data from other sensors such as TM and SPOT.

The formula used for the transformation of raw DN values into exoatmospheric reflectance (*EREF*) was developed in the study of Lake Chicot in Arkansas by Schiebe et al. The first step in the operation was the calculation of in-band radiance (L_λ) which is dependent on spectral radiance (L_λ) and the band-width for each MSS band (BW). The

band-widths used were those published in Table 6 of Landsat Technical Notes (Markham and Barker, 1986), which is found on page 30 in the Methodology chapter of this thesis.

Integrated in-band radiance was calculated as follows:

$$L = (BW)(L_{\lambda})$$

Spectral radiance (L_{λ}) was found for each band using the following equation:

$$L_{\lambda} = LMIN_{\lambda} + \left(\frac{LMAX_{\lambda} - LMIN_{\lambda}}{QCALMAX_{\lambda}} \right) (QCAL)$$

where $QCAL$ is the digital number, $LMIN_{\lambda}$ and $LMAX_{\lambda}$ are the post-calibration dynamic range of spectral radiance. $QCALMAX_{\lambda}$ is the range of the rescaled radiance in digital numbers (Markham and Barker, 1986), or the maximum number of gray levels that is sensed in each band. $LMIN_{\lambda}$ represents the spectral radiance sensed when the DN is 0, and $LMAX_{\lambda}$ is the spectral radiance when the DN = $QCALMAX_{\lambda}$. Figure 3 shows the radiometric response function found using the above equation for spectral radiance (Lillesand and Kiefer, 1994).

The final equation for the calculation of exoatmospheric reflectance using in-band radiance is as follows:

$$EREF = \frac{(\pi)(L)}{(SSI)(Ecc)(\sin\{ELV\})}$$

where SSI is the solar spectral irradiance at the top of the atmosphere for the corresponding Landsat satellite and the MSS band-width, Ecc is the eccentricity

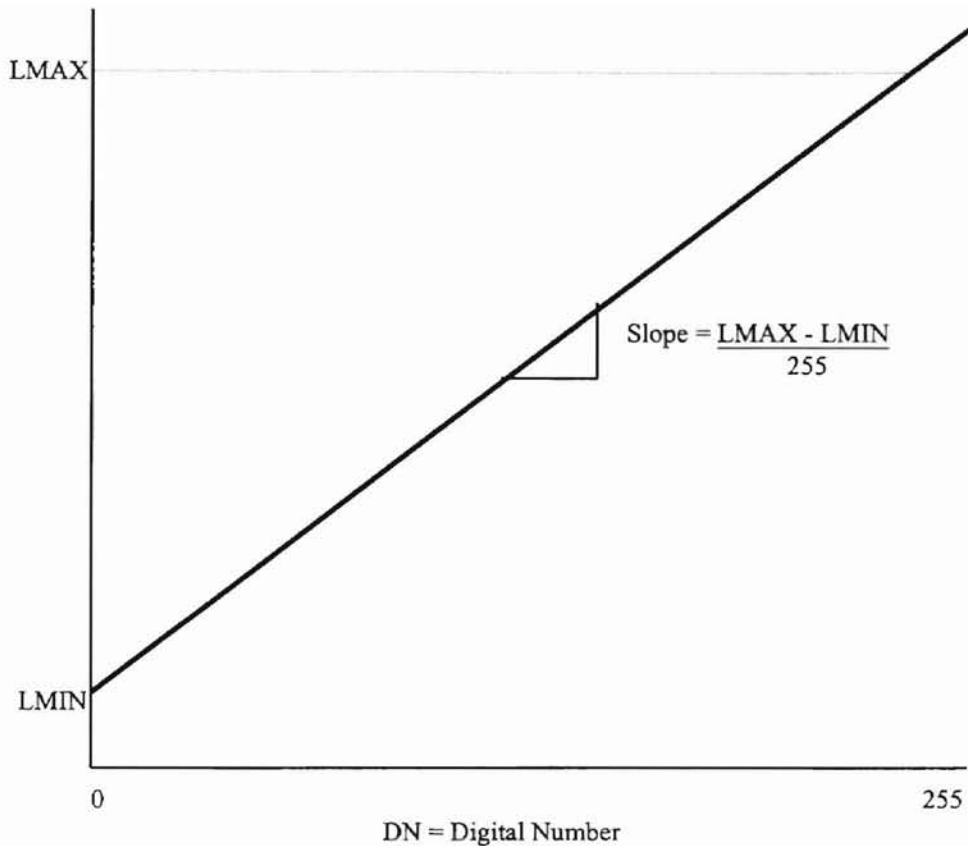


Figure 3. Radiometric response function (Lillesand and Kiefer, 1994).

correction factor, and ELV is the sun elevation angle (Schiebe et al., 1992). The values for solar spectral irradiance used were based on the spectrum recommended by the World Radiation Center (Iqbal, 1983). The eccentricity correction factor (Ecc) is:

$$Ecc = 1.000110 + (0.034221)(\cos\{DA\}) + (0.001280)(\sin\{DA\}) \\ + (0.000719)(\cos\{2DA\}) + (0.000077)(\sin\{2DA\})$$

where the day angle (DA) in radians is:

$$DA = (2)(\pi)(d - 1)/365$$

and where the day number (d) ranges from 1 on January 1st to 365 on December 31st (Iqbal, 1983).

Multispectral Dimension Reduction

A land cover classification that is derived from a single date is rarely complete for all cover types present during a growing season. In order to create multitemporal classifications, it is possible to simplify multispectral images through transformations which minimize the extraneous data present in multi-band data sets, thereby simplifying multidimensional data and minimizing processing. Transformed data from different times and sources can then be more effectively combined and analyzed. Many transformations have been developed to emphasize a wide range of features existent in multispectral imagery. Some techniques which are useful for land cover analysis and are to be discussed in this section include difference vegetation indices, the Tasselled Cap, and principal components analysis (PCA), among others.

The dimensionality of multi-band images can be reduced through the transformation of imagery into a one-band vegetation index. This process reduces the amount of data but retains useful information which indicates levels of plant growth (Kauth and Thomas 1976). A vegetation index is an image which displays pixels on a gray-scale where higher DN values represent more vigorous plant growth; that is, areas which appear black have little or no plant life and brighter pixels indicate the presence of

plant life. One example of such an image is a normalized difference vegetation index (*NDVI*), which is a ratio of near infrared (*NIR*) and visible (*VIS*) bands of a multispectral image:

$$NDVI = \frac{(NIR - VIS)}{(NIR + VIS)}$$

The result of this calculation can range between -1 and 1, where higher values indicate greater vegetation vigor.

The Kauth-Thomas Tasseled Cap transformation was specifically developed for identification of agricultural crop growth stages. The following discussion is a simple explanation of the Tasseled Cap transformation, which part of the transformation was used, and how the output of that operation is useful to this classification method.

When a single field planted with a given crop is remotely sensed a number of times throughout the growth and maturity of the crop, a pattern emerges that can be graphically represented on two-channel scatter plots. Before the emergence of the crop, the field has a bare soil response which, when displayed on a scatter plot of MSS Band 4 versus Band 2 appears as a diagonal line along which lies the mean reflectance of soils from light to dark, called the soil line. As the crop grows and gets greener, the near-infrared (*NIR*) reflectance increases which, on the scatter plot, draws the bulk of the pixels toward a point that is higher in Band 4 and lower in Band 2, or up and to the left. As growth reaches its peak, all pixels converge toward this point, creating a triangular shape like a woolen cap. When the crop begins to mature, reflectance for both Bands 4 and 2 is higher, which draws the pixels on the scatter plot up and to the right. This is the

“foldover” or the beginning of the tassels of the cap. As the crop gets yellower, the foldover increases and starts to drawdown the *NIR* reflectance and the scatter plot tends

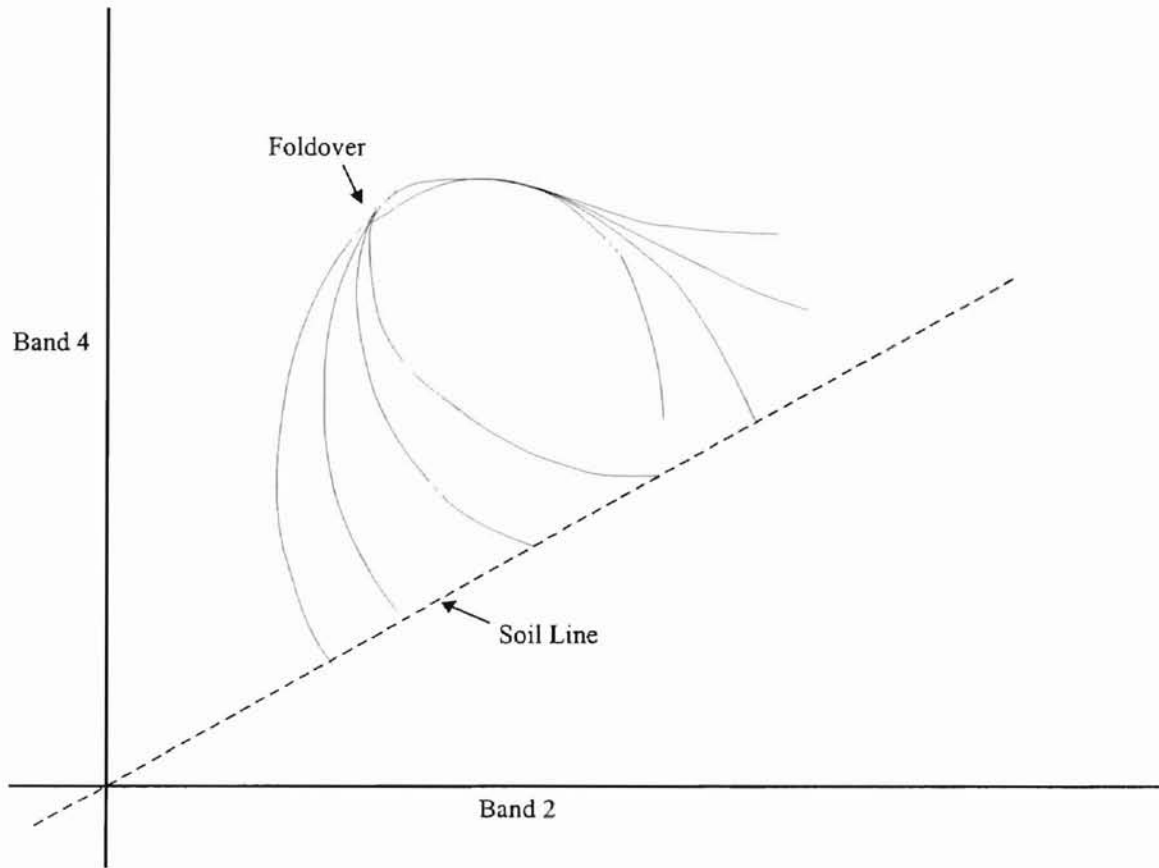


Figure 4. The Tasselled Cap (Kauth and Thomas, 1976).

back toward the soil line “from whence it came” (Kauth and Thomas, 1976). This forms the completion of the tasselled cap shape on a scatter plot in two dimensions. MSS images contain four bands, so this shape would exist in four dimensions, which is difficult to visualize.

The actual transformations of the image are algebraic expressions which rotate the axes of the four-dimensional space in which the image pixels are found. These rotations correspond to the directions determined by the tasselled cap shape described before. The

first transformation rotates the axis in the direction of the diagonal soil line, which results in an image which displays a feature called brightness. The second transformation is determined by an axis which is orthogonal to the soil brightness axis, and is called greenness, or a greenness vegetation index (Kauth and Thomas, 1976):

$$\text{GVI} = -.290(\text{Band 1}) + -.562(\text{Band 2}) + .600(\text{Band 3}) + .491(\text{Band 4})$$

The image produced by this transformation displays the level of green vegetation growth and represents the triangular cap part of the tasselled cap shape.

Principle and canonical component analyses are similar to the Tasselled Cap method in that they also perform a linear transformation of a multispectral image's axes. Images generated by different bands often appear to contain the same information due to interband correlation. These transformations are designed to reduce or remove such redundancy and compress the information into a new set of channels, or components, which are fewer in number than in the original data (Avery and Berlin, 1992). The tasselled cap transformation uses the same concept, but its components are determined by finding a spectral soil line as described above. A principal component analysis is performed by rotating the coordinate axes in spectral space according to the line along which the greatest variance is found. That axis is the first principal component, from which the second component is determined by an axis that is orthogonal to the first and whose data shows far less variance and therefore less information. Additional orthogonal components are determined for as many bands as are present in the original image, but each succeeding component contains far less information.

Canonical component transformations also define new coordinate axes, but are used when particular areas of interest contain known different feature types. The canonical component axes are rotated in order to maximize class separability and minimize the variability within those classes. This process also results in new components whose subsequent images contain lesser amounts of additional information (Avery and Berlin, 1992). The Tasseled Cap is a similar transformation but is based on agricultural crop cover.

The Tasseled Cap transformation was used in this study because it was developed specifically for agricultural applications. As the result of a linear transformation of all four MSS bands, the Kauth-Thomas GVI contains more information than a two-band NDVI ratio and is a more useful representation of ground cover. Also, resulting values in an NDVI tend to polarize towards very high or low ends of the range, whereas the distribution of values in a Greenness Vegetation Index tend to be more normal (Lo et al., 1986). The principal or canonical components analysis techniques were not used because the resulting information may or may not have been based on the same variations between bands in different images.

Studies Involving Multitemporal Land Cover Dynamics

Various procedures exist which can be used to monitor land cover change and it is generally accepted that different methods produce different maps of cover change (Singh, 1989). Several applications will be reviewed here that operated on the basic premise that

land cover changes are the greatest factor responsible for radiance changes detected by remote sensors on different dates.

One method for detecting land cover change using multitemporal imagery is to create single-date classifications for different years and compare each separately. One such application used Landsat MSS and TM data from six years in an investigation of tropical forests in Brazil to find patterns of forest regrowth over time (Lucas et al., 1993). A time-series of Landsat data was required to classify various stages of regrowth that would have similar spectral signatures on a single-date image. The objective was to determine the age of secondary forest by analyzing the biomass accumulation of the regrowth. The dates of acquisition of the TM scenes used were 1985, 1988, 1989, and 1991, all in the summer. The images were all geometrically registered to the 1991 scene. A supervised classification method was used with reference data from 60 training sites representing only three broad land cover types: primary forest, secondary forest, and agricultural land. Each image was classified separately and examined for land cover changes according to each pixel location over the six-year period. The accuracy of the classifications was to be tested at a later date, but a problem was encountered with the “inability to adequately discriminate plantations from secondary forest” (Lucas et al., 1993).

A similar investigation was performed by Howarth and Boasson (1983) using MSS data for change detection in the urban environment of the city of Hamilton in Ontario, Canada. This study used only two dates, 6 July 1974 and 12 July 1978. The single-date classification method was rejected in favor of enhancement procedures using both dates which could better identify land cover changes. Three enhancements were

used: an overlay of band 2, ratios of bands 2 and 4, and a vegetation index. The first enhancement overlaid band 2 from both images and displayed the 1974 image in green and blue on a CRT monitor, and the 1978 image in red. Areas that had changed in cover were highlighted in one of the colors while gray pixels represented no change. The next method ratioed one band from the first image with the same band from the second image. The result gave areas that had no change a ratio of 1.0 which were displayed as a medium gray tone. Areas of changed cover were identified in lighter or darker tones, with the level of intensity indicating the extent of change. The results from NDVIs performed on both dates were also overlaid and displayed using different color guns. This process identified areas that had experienced changes in vegetative cover.

All three enhancement methods were successful in locating areas that had undergone land cover changes, which was generally based on vegetation presence or nonpresence due to new construction. In this instance, the enhancements described were sufficient for locating areas that had undergone the basic change from nonurban to urban. However, identifying land cover change on a broader scale including agricultural land requires a more extensive classification procedure due to varying spectral signatures for different plants and growth states.

Lambin and Strahler (1994) described a successive-year change detection process for Advanced Very High Resolution Radiometer (AVHRR) data using a change-vector analysis. Their study investigated the nature and magnitude of land cover change in West Africa using high temporal-resolution data. Instead of using individual classifications from different years, they based their method on a "comparison of the temporal development curve, or time-trajectory, for successive years," using multiple NDVIs from

100 AVHRR images acquired throughout a two-year period. The change vector measured the intensity of the changes in NDVI values between each pixel in multi-dimensional space. This approach represents a simultaneous analysis of multitemporal data that was able to detect subtle land cover changes within a class both during one growing season and from year to year (Lambin and Strahler, 1994).

A study using multitemporal AVHRR data was conducted to analyze “dynamic processes of terrestrial vegetation” in Africa (Holben, 1986). The objective of this investigation was to use multirate imagery to simulate a single date rather than observe land cover change over years. Composites were created based on NDVIs from a series of georeferenced multitemporal AVHRR images from seven successive days. The procedure was called a maximum-value composite (MVC), where each NDVI value was examined on a pixel-by-pixel basis and only the highest value was kept, resulting in a single-band image essentially representing a single date. This process was performed in order to minimize problems that are inherent to single-date acquisitions such as cloud cover and atmospheric attenuation. The MVC technique was found to be effective for producing suitable images for observing land cover dynamics.

A land cover change detection process based on one growing season would have the ability to identify different agricultural crops being produced and specify which parts of the season those crops were being grown in during that year. This concept was demonstrated by Hlavka et al. (1979) in a study of a multitemporal classification of winter wheat in Kansas. Their objective was to use a growth state model to create crop signatures that represent specific levels of maturity of winter wheat. MSS data from five observation times was transformed using Kauth-Thomas greenness coefficients into a

vegetation index from which growth state signatures were derived using an iterative clustering technique. A category signature was found for each band and growth state for each observation based on the mean spectral reflectance in a small patch of winter wheat. The initial mean signature for a category was run through an iterative procedure with successive growth states and observations which results in a final mean signature for each observation. Using field verification of the wheat, classification results were 85% correct when using a signature based on 36 growth states and 79% correct using a 5 growth state signature. These conclusions emphasize the conclusion that increasing points of observation improves the accuracy of multitemporal land cover studies.

A study undertaken by Lo et al. (1986) used a method of multitemporal land cover classification that is most similar to the one used in this study. MSS imagery representing the Green Bay, Wisconsin area for the 1979 growing season was used to compare single-date and multitemporal classification approaches and to evaluate a number of supervised and unsupervised classification techniques. The dates chosen to represent different stages in a growing season were 20 May, 25 June, 5 July, and 6 September and were all cloud free and of good quality. Field surveys of the study area were also conducted to verify crop development. Radiometric correction of the images was performed to normalize solar illumination conditions. The tasselled cap transformation was used to isolate measures of greenness, and band ratios and principal component transformation were also used for data compression. The field verification data available made it possible to use both unsupervised and supervised classification techniques.

The best results for multitemporal unsupervised classifications obtained in the Lo et al. study in terms of overall accuracy were found with a band 4/band 2 ratio (85.7%) and the GVI transformation (83.9%). The accuracy was determined by an error matrix comparing the ground reference data with the actual number of pixels occurring in each class. The discrepancies between the classifications and reference data were attributed to inseparability of the multitemporal profiles of some of the known ground covers, errors in the location or interpretation of ground reference points, and misregistration of the multitemporal images.

Comparisons between the multitemporal and single-date classifications revealed a definite advantage in multi-date analysis. The September scene was classified using the same unsupervised method and resulted in an accuracy of 66%. It was found that certain features were not spectrally separable using a single date; the spectral reflectance of woodland was identical to corn at that point in the growing season. As a result, 30 out of 51 pixels which should have been classified as woodland were assigned to the corn class. The unsupervised analysis of the band ratio images resulted in nine land cover classes: woods, pasture/grass, corn, alfalfa, oats, bare soil, water, impervious surfaces, and mixed, which represents pixels containing more than one land cover type. The increased ability to identify specific crops using a multitemporal approach was well illustrated in the study (Lo et al., 1986).

Accuracy in the Registration of Overlaid Images

The importance of image registration to the accuracy of a multitemporal land cover classification was also mentioned in the Lo et al. (1986) study. Any misregistration in a set of overlaid images will result in incorrect data in that a given pixel in each image represents a different area on the ground. For instance, a physical feature such as a field boundary may be offset between images so that there appears to be more than one boundary. This offset would show that a pixel which represents an vegetative cover on one image would display a different ground cover on the same pixel in an overlying image. In a multitemporal composite this would be interpreted as a change in land cover because of the different spectral response in each pixel. Howarth and Boasson (1983) also stated that “inaccuracies can be introduced by misregistration on the two images being compared” in their study of change detection in urban environments. An accurate geographic referencing of each scene that is to be overlaid makes it possible to avoid this problem. Holben’s (1986) maximum-value composite of multitemporal AVHRR imagery was also affected by misregistration. AVHRR registration is “dependent on the accuracy of location information embedded in the data”, which is dependent on the data’s source. Some location error occurred in their study, but the very large viewing area represented by AVHRR data did not present a serious problem, and was corrected using control-point rectification.

The imagery used in this study represented a much smaller area of land and a higher spatial resolution than AVHRR data and required a much more accurate registration. This was accomplished using a geometric rectification procedure that

resampled each image, assigned geographic coordinates to each pixel, and assured that each image was registered correctly.

CHAPTER THREE

METHODOLOGY

Chapter Overview

This chapter describes the procedure developed in this study for the creation of a land cover classification of multitemporal Landsat MSS data based on changes during a growing season. This method of land cover change detection is a simultaneous analysis of multitemporal data similar to the approaches used by Lambin and Strahler (1994) and by Lo et al. (1986). However, the change detection process for this study was based on a comparison of temporal development during one growing season rather than Lambin and Strahler's objective of obtaining indications from successive years.

The procedure consisted of the transformation and integration of three MSS scenes from one year resulting in one image which indicated the land cover changes during the year. That image was then analyzed and classified in multitemporal land cover classes. The growing season for one year was represented by one MSS scene each from spring, summer, and fall. After being radiometrically and geometrically corrected, these scenes were transformed using the greenness coefficients from the Kauth-Thomas Tasseled Cap Transformation. Each scene was converted to a single-band greenness vegetation index which displayed varying intensities of plant growth, and was then overlaid in a three-band image and displayed as a composite.

This composite image displayed the multitemporal land cover changes that were present in the three MSS scenes. Bands 1, 2, and 3 of the composite were represented by, respectively, the spring, summer, and fall greenness indices and were displayed with band 1 in red, band 2 in green, and band 3 in blue. The colors resulting from the combinations of the pixel DN's of the indices indicated levels of plant growth at the three distinct points in the growing season.

The three-band composite was then processed using an unsupervised classification resulting in a specified number of spectral clusters. The classification procedure was performed using output images consisting of forty, fifty, and sixty clusters. The fifty-cluster image was found to be most effective, as forty clusters did not separate similar cover types sufficiently and sixty clusters revealed no more useful separability than did fifty. Using image interpretation techniques, aerial photographs, topographic maps, and some field verification, these clusters were grouped into classes representing the land cover of the region. The classes differed from those used for conventional classifications (those not using multitemporal data in one image) due to the need for classes depicting seasonal variations and the nature of the output from the linear greenness transformation. This issue and the entire method of image processing and classification will be examined in detail in this chapter. The determination of the land cover in each classification for each year will be discussed in the Analysis and Results chapter.

As mentioned in the Introduction, the methods developed in this study will be applied to other sources of multispectral imagery, notably Thematic Mapper and SPOT, in research after this study. Every operation described in this chapter can be performed

on TM and SPOT images, including the derivation of the greenness vegetation index, for which coefficients have been developed for use with those alternative sources. However, the image types cannot be combined for use in the same classification due to the differences in spatial resolution.

The methodology involved with this study consisted almost entirely of image processing executed with Erdas software, specifically, PC Erdas 7.5 and Erdas Imagine 8.0. The operations performed included image loading, subscene isolation, radiometric correction, geometric correction, delineation of the Little Washita Watershed, Kauth-Thomas greenness vegetation index transformation, combination of the three indices into a three-band composite images, and unsupervised classification of those images. Since field verification was impossible for this research, aerial photographs, topographical maps, and “windshield surveys” of land cover were used to draw basic conclusions regarding the structure of the landscape at the field level. That issue will be described in detail in the Analysis and Results chapter.

Image Loading and Subsetting

Every MSS image used in this study was delivered on 9-track computer-compatible tape (CCT) on which a full scene was recorded. The format used to record the data on the tape and, therefore, to retrieve the data varied according to the date of acquisition. Landsat 1 MSS scenes used a band-interleaved-by-pixel (BIP) format called X-Format and consisted of four separate images which represented a full scene that was divided into four columns. Scenes from Landsats 2 and 3 were also divided into four

sections, but these were in band-interleaved-by-line (BIL) format. The other two satellites used a band sequential format where the full scene of each band was recorded as a separate file on the tape. PC Erdas allows for the loading of each of these formats using the LOADX and LDDATA (Load Data) modules. The following is a description of the steps used to load and process one image from a CCT.

To save hard disk space on the computer and image processing time, a subset of the full scene which included the study area was loaded from tape. Using the PREVIEW module, it was possible to view the full scene on the tape and determine the coordinates needed to define a subscene which includes the area needed. The upper left and lower right corner pixels of the subset desired were located and their X and Y file coordinates on the tape were noted and used to load the study area to a single four-band file on the hard disk. For the X-Format images the study area was defined from the full scene using the SUBSET module.

Radiometric Correction

The need to normalize the image data used in this study, having been acquired by five different satellites and with varying solar illumination conditions, was explained in the Literature Review chapter. The raw image data were converted to exoatmospheric reflectance (*EREF*) using the formula developed by Schiebe et al. (1992). This process was executed using the ALGEBRA module. The *EREF* formula was applied to every pixel in each band in the raw MSS image, resulting in another four-band image whose DN's represented exoatmospheric reflectance. Since the output of the equation was a

measure of reflectance, which was a percentage that ranged between 0 and 1, it was necessary to apply a scalar of 200 to better utilize the 8-bit file structure in PC-Erdas. This structure consisted of 256 gray levels and only stored DNs as integers. Below is the *EREF* formula as it was used in ALGEBRA for each of the four MSS bands:

$$EREF = \left\{ \left((\pi) * (BW) * (LMIN + ((LMIN - LMAX) / QCALMAX) * X) \right) / (SSI * Ecc * \sin(ELV)) \right\} * 200$$

where *BW* is the bandwidth (shown in Table II, taken from Markham and Barker, 1986), *LMIN* and *LMAX* determine the post-calibration dynamic range of spectral radiance (shown in Table III, taken from Markham and Barker, 1986), *QCALMAX* is range of digital numbers representing rescaled radiance, *X* is the digital number, *SSI* is the solar spectral irradiance (shown in Table IV, taken from Schiebe et al., 1992), *Ecc* is the earth's

TABLE II
LANDSAT MSS SPECTRAL BANDS

BAND	MSS 1		MSS 2		MSS 3		MSS 4	
Satellite	Band-Pass (μm)	Band-Width (nm)	Band-Pass (μm)	Band-Width (nm)	Band-Pass (μm)	Band-Width (nm)	Band-Pass (μm)	Band-Width (nm)
"Nominal" Specification	.5 .6	100	.6 .7	100	.7 .8	100	.8 1.1	300
Landsat 1	.4968 .6050	108.2	.5988 .7068	108.0	.6885 .8086	120.1	7909 1.0326	241.7
Landsat 2	.4943 .6027	108.5	.6036 .7164	112.8	.6909 .8108	119.9	7896 1.0323	242.8
Landsat 3	.4939 .5991	105.1	.6026 .7105	107.9	.6872 .8003	113.1	.7966 1.0185	221.8
Landsat 4	.4921 .6094	117.3	.5998 .7006	100.9	.6954 .8129	117.5	.7903 1.0637	273.5
Landsat 5	.4947 .6109	116.2	.6001 .6990	98.8	.6985 .8148	116.3	7937 1.0690	275.2

(Markham and Barker, 1986)

TABLE III
 LANDSAT MSS POST-CALIBRATION DYNAMIC RANGES FOR
 U.S. PROCESSED DATA
 SPECTRAL RADIANCES, LMIN AND LMAX
 (in $\text{mW} \cdot \text{cm}^{-2} \cdot \text{ster}^{-1} \cdot \mu\text{m}^{-1}$)

BAND	MSS 1		MSS 2		MSS 3		MSS 4	
Satellite	LMIN _{<i>λ</i>}	LMAX _{<i>λ</i>}	LMIN _{<i>λ</i>}	LMAX _{<i>λ</i>}	LMIN _{<i>λ</i>}	LMAX _{<i>λ</i>}	LMIN _{<i>λ</i>}	LMAX _{<i>λ</i>}
Landsat 1 ALL	0.0	24.8	0.0	20.0	0.0	17.6	0.0	15.3
Landsat 2 < 7/16/75	1.0	21.0	0.7	15.6	0.7	14.0	0.5	13.8
> 7/16/75	0.8	26.3	0.6	17.6	0.6	15.2	0.4	13.0
Landsat 3 < 6/1/78	0.4	22.0	0.3	17.5	0.3	14.5	0.1	14.7
> 6/1/78	0.4	25.9	0.3	17.9	0.3	14.9	0.1	12.8
Landsat 4 < 8/26/82	0.2	25.0	0.4	18.0	0.4	15.0	0.3	13.3
8/26/82 - 3/31/83	0.2	23.0	0.4	18.0	0.4	13.0	0.3	13.3
> 4/1/83	0.4	23.8	0.4	16.4	0.5	14.2	0.4	11.6
Landsat 5 < 4/6/84	0.4	24.0	0.3	17.0	0.4	15.0	0.2	12.7
4/6/84 - 11/8/84	0.3	26.8	0.3	17.9	0.4	15.9	0.3	12.3
> 11/9/84	0.3	26.8	0.3	17.9	0.5	14.8	0.3	12.3

(Markham and Barker, 1986)

TABLE IV
 LANDSAT MSS SOLAR SPECTRAL IRRADIANCE VALUES
 (in $\text{mW} \cdot \text{cm}^{-2}$)

Satellite	MSS 1	MSS 2	MSS 3	MSS 4
Landsat 1	20.060	16.991	15.373	21.520
Landsat 2	20.138	17.486	15.274	21.648
Landsat 3	19.870	19.592	16.845	14.619
Landsat 4	23.682	21.730	15.942	14.854
Landsat 5	23.626	21.488	15.688	14.614

(Schiebe et al., 1992)

eccentricity factor, and *ELV* is the sun elevation angle. Each of these variables changed for each band except the *Ecc* and *ELV*, which were determined by the date of the scene's acquisition and remained constant in all four calculations.

Geometric Correction

A geometric correction was performed on each image to rectify the distortion inherent in MSS imagery due to the satellite's altitude, attitude, and velocity, as well as other factors such as earth curvature, relief displacement, and panoramic distortion, among others (Lillesand and Kiefer, 1994). This correction gave the image the geometric integrity of a map and referenced each pixel to real-world coordinates which was necessary for the delineation of the Little Washita Watershed, which will be discussed later. The process of geometric correction required the location of ground control points (GCPs) in the image. These GCPs were places which were accurately located and identified on the image, such as road intersections, and had a known ground location. A set of 83 GCPs in and around the Little Washita Watershed were located specifically for this study and their Universal Transverse Mercator (UTM) grid coordinates determined using USGS 7.5 minute quadrangles. The minimum number of controls points needed to perform a geometric correction is generally around 60. About 75 GCPs were found in each subset image and both their UTM and X,Y coordinates in the raw image were recorded using the GCP module.

The GCPs were transformed into an output raster grid defined by the UTM coordinates using the COORDN module, which performed a multiple regression analysis

using the GCPs' image and UTM coordinates, and the root means squared (RMS) error was calculated. The RMS error was based on each GCP's accuracy according to its UTM, or real-world, location and its relationship to the other GCPs, and the size of the pixels in the images. An error greater than 1% indicated that a pixel in the output grid would be more than one pixel's width away from its true ground location. If the RMS error was above 1%, the GCP with the highest contributing error was removed from the set and the RMS error was recalculated. This process was repeated until the RMS error was below 1%, and an accurate output grid was defined by the coordinate transformation.

A resampling function was then carried out by the LRECTIFY module which transformed the distorted image into a geocorrected image according to the grid created by the coordinate transformation. The output image was georeferenced so the top of the image represented true north. The resampling technique used was a nearest neighbor assessment, which assigned a DN for a pixel in the geometrically correct output matrix based solely on the DN of the nearest pixel in the distorted input matrix. This method resulted in features that may appear disjointed in the output image, because the output location can be offset by up to one-half pixel. However, this method left the original DN value unaltered, which was important for this study, as comparisons between years depended on the exoatmospheric reflectance value. The other available resampling techniques, bilinear interpolation and cubic convolution, result in an output DN calculated by a given pixel's surrounding pixel values (Lillesand and Kiefer, 1994).

The subset image represented an area larger than the watershed, including land west and north of the study area, throughout which the 83 GCPs were evenly distributed. This insured an accurate transformation while eliminating the need to geocorrect a full

MSS scene. For this study, the watershed was required to be identified and separated from the subset as a distinct image. In order to delineate the Little Washita Watershed from the corrected subscene, a separate file was created using the CUTTER module and a polygon file representing the watershed boundary extended out by 500 meters. The resulting image was in the shape of a rectangle, but every pixel that lay outside the watershed buffer polygon had a DN value of zero and was displayed as black.

The importance of the accuracy of the geometric correction has been explained and was checked by overlaying the three images from one year and visually inspecting the images' registration. An error of one pixel was easily recognized and was corrected by adjusting the file coordinates of the uncorrected image that did not overlay properly with the other two. If such errors were found, the rectification process was then performed again until all three overlaid correctly.

Derivation of the Greenness Vegetation Index

The next step in the process called for the compression of the four-band MSS data. The Kauth-Thomas Greenness coefficients described earlier were applied to each watershed image, reducing the dimensionality of each image. As with the radiometric correction, this process was also performed with the ALGEBRA module. An output file representing a greenness vegetation index resulted from the operation. Each pixel was subjected to the following formula according to that pixel's DN value in each of the four bands:

$$GVI = -.290*(X1) + -.562*(X2) + .600*(X3) + .491*(X4)$$

where X represents the pixel's DN for that band number and GVI is the output pixel's greenness value. The program was directed to scale the resulting values by adding 10 and then multiplying by a factor of 3 to effectively spread the DNs through the range of the 8-bit output file. This was a necessary step because the DNs in the image were stored as integers and a larger degree of precision was needed since the unscaled output derived from the exoatmospheric reflectance data usually had a minimum value of -10 and a maximum value around 50. After being scaled, the GVI was represented by a range from 0 to about 150, which afforded a better indication of variations in ground cover according to vegetation vigor.

GVI Composite Construction and Interpretation

To create a land cover classification for one year that included three separate MSS scenes, an image was created by transforming the information contained in those scenes into a single image. This was accomplished by converting each four-band image into a one-band image and combining the three into one scene. A Kauth-Thomas Greenness transformation was applied to each image, which created a one-band file from a four-band MSS file, containing an image representing a greenness vegetation index.

As mentioned before, a false-color composite was created by placing each single-band greenness vegetation index into a three-band file where the spring index was band 1 and displayed in red, the summer index was band 2 and displayed in green, and the fall index was band 3 and displayed in blue. This operation was performed using the SUBSET module. The resulting image was very useful for determining crop growth

states throughout a growing season. Figure 5 shows the GVI composite for 1988. In such a scene, an area having high greenness, or vigorous plant growth, in one band of the image (during one part of the season) and low greenness in the other two bands (the rest of the season), appeared brightly in the color assigned to that band. For example, over the course of one year, a field planted in winter wheat would have vigorous growth in the spring, would be bare in the summer after harvesting, and may be left fallow in the fall. This field would appear bright red on the false-color GVI composite. Accordingly, bright green areas would represent fields with high greenness in summer and no growth in the spring and fall. Bright blue areas would be fields showing growth in the fall and none in the spring and summer.

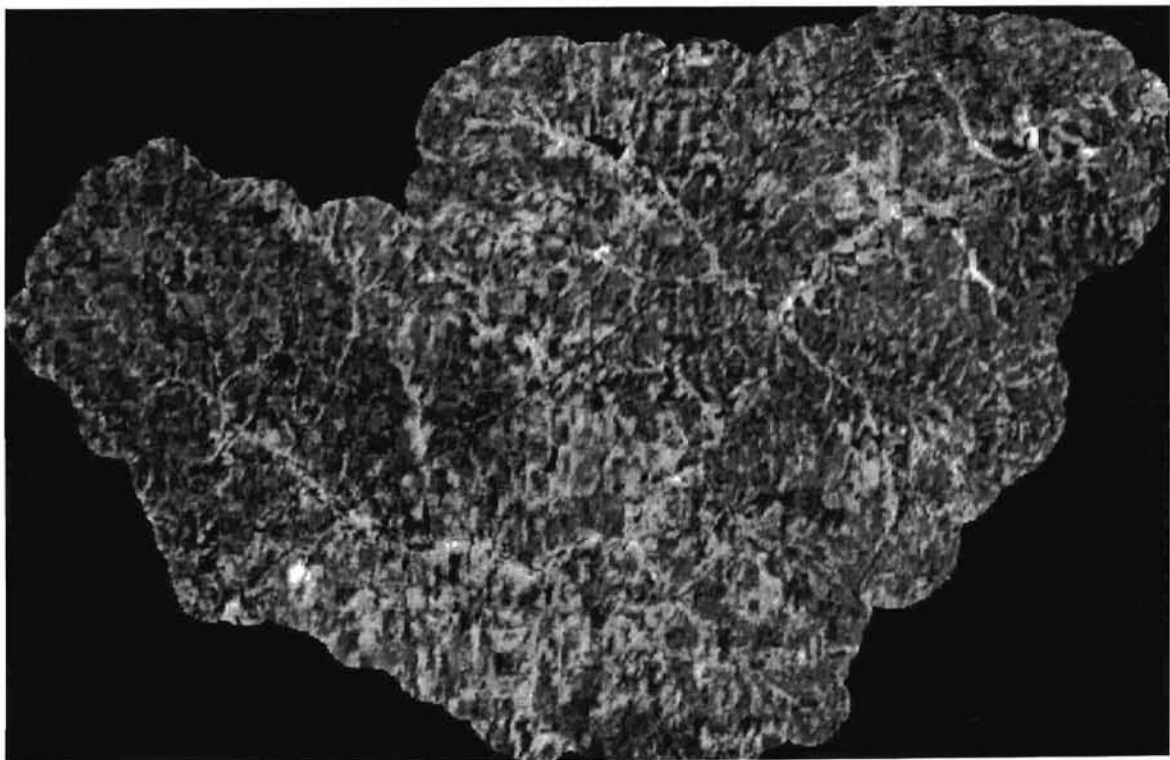


Figure 5. False-Color Composite of 3 GVIs -May, June, & November, 1988

Further conclusions were made from other colors in the image with the use of the additive color process, that is, different colors of light superimposed. When red and blue light were combined, as they were when an area in both the spring and fall bands of a composite showed high greenness, the resulting color was magenta. Mixtures of red and green were yellow, and cyan resulted from mixing blue and green. All colors superimposed resulted in white, which represented areas with high greenness values in all three seasons. Through interpretation of the GVI composite, it was possible to differentiate between crop types and which seasons and years those crops were produced, which leads to the discussion of the classification process.

Unsupervised Classification of the GVI Composite Image

Land cover classifications are produced by categorizing every pixel in an image into distinct classes. This is done by grouping pixels into clusters based on spectral response and pattern recognition. Spatial and temporal patterns are important indicators of land cover (Avery and Berlin, 1992), especially for the data set used in the research described here. Spatial patterns are drawn from image pixels' relationships with surrounding pixels, such as delineating an agricultural field based on its shape and image texture. Temporal patterns are those which are based on the number of images used and the time spanned between acquisitions. These indications and the multitemporal data set used here allowed for the discrimination of pixels representing crops grown at various times in a growing season.

The method of classification used was an unsupervised classification. This process consisted of two steps: the image was classified into natural spectral clusters which were then grouped into land cover classes based on ground reference data. An unsupervised classification works on the premise that the data in the image can be separated into distinct spectral groups which represent different types of land cover. The data in these groups are assumed to be related closely in the spectral measurement space, while the groups themselves should be well separated from each other spectrally (Hord, 1986). Forty of these clusters were found for the Little Washita images. These clusters were determined by the ISODATA module using an algorithm called the "K-means" approach, where arbitrary mean vectors were determined in spectral space for forty groups, then each pixel was assigned to the nearest vector, and new mean vectors were calculated and another iteration was performed. The procedure was repeated until all pixels had been classified into groups that showed no significant change in the location of their mean vectors between successive iterations.

An unsupervised classification is dependent upon ground reference data on which to base the determination of land use classes and how the forty clusters will be assigned to those classes. Field verification was, of course, impossible for the dates of the imagery used in this study. However, ancillary ground reference data was available for the Little Washita Watershed in the form of topographic maps, aerial photographs taken in 1968, TM and SPOT scenes, and extensive "windshield surveys" done in 1992 and 1994. This information was used to draw conclusions on the historic locations of features such as agricultural fields, wooded areas, and different qualities of rangeland. These features were used to group other areas with similar spectral responses into the same class. Other

image interpretation techniques such as shape, texture, site, and association recognition were used to find spatial patterns in the images.

CHAPTER FOUR

ANALYSIS AND RESULTS

Methodology of Analysis

The output image from the unsupervised classification was a one-band file which consisted of forty clusters. The next step was to group those clusters into classes which represented the land cover present in the three images depicted a growing season. This required the analysis of each cluster's spectral signature and the interpretation of the appropriate cover from those signatures. The image was then recoded as a land cover classification in which each pixel was assigned to one of the land cover classes used in this study.

The land cover classification was based on classes determined by the multitemporal nature of the data set. As mentioned earlier, a standard classification uses classes that may not differentiate between spring, winter, and fall crops such as winter wheat and summer crops such as alfalfa or corn. When determining a classification process, it is necessary to allow for the inclusion of all parts of the study area and provide a unit of reference for each land cover type (Anderson et al., 1976). The classes that were used for this research were defined both by the types of land cover present in the watershed and the multitemporal data. The combination of images acquired at three different times during a growing season (spring, summer, and fall) created a unique set of

land cover classes based on the presence of crops at those times. The composite described earlier generated the following agricultural classes:

- Winter Wheat - Spring Only
- Winter Wheat - Fall Only
- Winter Wheat - Spring and Fall
- Summer Crops
- Spring and Summer Crops
- Summer and Fall Crops
- Spring, Summer, and Fall Crops

The other land cover classes used were those determined by the National Agriculture Water Quality Laboratory for their Washita '92 project and included the following:

- Water
- Urban/Highways
- Bare (Bare soil, quarries, oil waste land)
- Native Rangeland
- Improved Rangeland (Pasture)
- Woodland

In a greenness vegetation index, those pixels having Water, Bare, and Urban/Highway responses all had very low values, because they represented areas with little or no vegetation. For this reason, those land cover types were combined into one class for this research.

The analysis of the spectral signatures and recoding of the land cover data was performed using Erdas Imagine. This software allows for statistical analysis of the separability of each cluster and graphical interpretation of signatures in feature space. In the case of this study, the spectral signatures were based on the greenness values in each of the three bands of the GVI composite. A feature space image plots a pixel's value in one band against its value in another band. In this way, each cluster was located in feature space according to the greenness level in each band and was compared with other

clusters' locations. This process was valuable for visualizing and grouping spectrally similar clusters into the same land cover class and determining the comprehensive signatures for each class.

Multitemporal Land Cover Class Spectral Signatures

Each of the forty clusters was assigned to a cover class through an interpretation process using the spectral signatures and spatial association techniques. The signatures created for each cluster are represented by the greenness value in each of the three bands in the GVI composite. This information was analyzed using the Signature Editor in Erdas Imagine. As in the composite source image, the signature averages were output as a red, green, or blue color according to the source image bands which represented spring, summer, and fall. The combinations of the averages for each season resulted in a distinct color just as in the GVI composite. Tables V-VIII list each cluster's signatures, the number of pixels, and the class assigned for each year used in this study.

The patterns created by the variations in greenness for each season were indicators of the type of land cover represented by each cluster. For example, a signature whose greenness values were fairly high in spring and summer but low in the fall was representative of a woodland's multitemporal response. A low response in the spring and fall but a little higher in summer was indicative of a rangeland signature. For this study, two rangeland classes were used: Native Rangeland and Improved Rangeland. The growth patterns for each class were similar, but Improved Rangeland was assumed to have shown a higher greenness response, as such a land cover would represent some type

TABLE V
CLUSTER SIGNATURE LISTING FOR 1976

Cluster	Count	Spring	Summer	Fall	Class
(1)	59548	0.054	0.034	0.052	Water, Urban, Bare
(2)	1672	12.434	5.136	54.616	Winter Wheat - Fall Only
(3)	1491	13.064	76.732	14.422	Summer Crops
(4)	3631	13.448	3.836	28.959	Native Rangeland
(5)	1163	14.025	84.415	43.046	Summer Crops
(6)	2872	14.271	111.931	18.065	Summer Crops
(7)	598	14.188	38.379	42.624	Native Rangeland
(8)	676	14.857	24.074	19.961	Native Rangeland
(9)	3739	14.902	46.774	16.465	Native Rangeland
(10)	2300	16.881	11.781	99.073	Winter Wheat - Fall Only
(11)	6712	18.312	114.539	66.212	Summer and Fall Crops
(12)	3459	18.349	57.923	56.877	Improved Rangeland
(13)	605	20.598	146.370	28.663	Summer Crops
(14)	3054	22.478	22.447	36.848	Native Rangeland
(15)	4129	22.924	60.234	34.184	Improved Rangeland
(16)	6487	24.377	3.232	13.120	Native Rangeland
(17)	5595	25.461	36.441	27.372	Native Rangeland
(18)	4323	29.824	45.812	39.191	Improved Rangeland
(19)	2454	30.905	28.947	55.940	Improved Rangeland
(20)	4068	32.379	3.054	37.523	Native Rangeland
(21)	2799	32.527	22.555	21.710	Native Rangeland
(22)	5630	33.751	78.162	70.077	Woodland
(23)	3363	34.466	45.518	77.126	Woodland
(24)	5659	34.707	48.224	53.316	Improved Rangeland
(25)	3733	35.989	70.643	46.669	Woodland
(26)	4738	37.414	48.162	20.516	Improved Rangeland
(27)	1236	37.598	30.950	39.094	Improved Rangeland
(28)	4946	39.315	3.189	62.966	Woodland
(29)	3348	41.209	99.696	43.758	Woodland
(30)	2681	42.207	73.921	25.131	Woodland
(31)	1400	43.678	1.552	10.575	Winter Wheat - Spring Only
(32)	2491	44.377	52.846	39.224	Improved Rangeland
(33)	2858	45.410	61.960	60.804	Woodland
(34)	634	53.528	81.992	59.956	Woodland
(35)	3064	54.325	103.883	79.490	Spring, Summer and Fall Crops
(36)	2332	54.824	40.408	57.011	Improved Rangeland
(37)	2383	57.440	35.387	29.772	Winter Wheat - Spring Only
(38)	989	58.267	3.036	35.461	Winter Wheat - Spring Only
(39)	349	58.369	6.114	126.683	Winter Wheat - Spring and Fall
(40)	2817	59.318	68.529	76.690	Woodland
(41)	1341	60.842	65.075	44.117	Woodland
(42)	1145	62.985	1.440	8.317	Winter Wheat - Spring Only
(43)	443	64.295	6.151	67.596	Winter Wheat - Spring and Fall
(44)	1035	80.247	71.701	136.425	Spring, Summer and Fall Crops
(45)	195	80.305	92.268	45.632	Spring and Summer Crops
(46)	90	88.273	2.024	11.092	Winter Wheat - Spring Only
(47)	83	105.218	123.711	67.699	Spring, Summer and Fall Crops
(48)	188	111.779	27.336	51.366	Winter Wheat - Spring and Fall
(49)	130	120.220	141.844	136.043	Spring, Summer and Fall Crops
(50)	85	150.243	150.583	53.010	Spring and Summer Crops

TABLE VI
CLUSTER SIGNATURE LISTING FOR 1984

Cluster	Count	Spring	Summer	Fall	Class
(1)	58817	0.029	0.024	0.022	Water, Urban, Bare
(2)	255	1.980	61.875	46.165	Water, Urban, Bare
(3)	213	4.446	2.596	43.901	Water, Urban, Bare
(4)	268	3.601	57.015	1.836	Water, Urban, Bare
(5)	80	23.363	19.575	101.325	Winter Wheat - Fall Only
(6)	756	35.459	33.767	23.044	Water, Urban, Bare
(7)	3763	45.739	44.089	42.238	Native Rangeland
(8)	2918	47.873	56.326	24.514	Native Rangeland
(9)	757	51.918	18.206	35.268	Water, Urban, Bare
(10)	5654	51.862	57.470	37.856	Native Rangeland
(11)	1896	52.397	82.459	35.627	Woodland
(12)	4757	55.261	44.534	31.771	Native Rangeland
(13)	665	56.123	138.277	60.370	Summer Crops
(14)	6573	57.947	56.389	51.790	Native Rangeland
(15)	2534	58.848	54.497	74.872	Improved Rangeland
(16)	4075	58.850	43.090	60.511	Improved Rangeland
(17)	4361	59.067	69.622	42.022	Woodland
(18)	6741	59.366	43.562	44.918	Native Rangeland
(19)	1619	59.562	101.053	52.463	Summer Crops
(20)	3207	60.622	73.828	60.809	Improved Rangeland
(21)	7598	64.464	54.202	37.640	Native Rangeland
(22)	1340	65.246	39.549	106.935	Winter Wheat - Fall Only
(23)	3531	66.932	67.518	28.651	Improved Rangeland
(24)	397	68.557	142.882	120.841	Summer and Fall Crops
(25)	5966	70.230	63.888	45.375	Woodland
(26)	2033	71.919	65.516	91.803	Improved Rangeland
(27)	1358	72.616	25.377	55.056	Winter Wheat - Spring and Fall
(28)	4908	72.996	48.910	50.470	Improved Rangeland
(29)	4258	74.164	58.761	62.435	Improved Rangeland
(30)	4887	74.541	81.387	40.634	Woodland
(31)	770	74.534	71.065	129.842	Winter Wheat - Spring and Fall
(32)	1089	75.112	102.798	88.955	Summer Crops
(33)	2826	77.372	39.383	75.437	Winter Wheat - Spring and Fall
(34)	2042	79.250	41.472	35.496	Winter Wheat - Spring Only
(35)	2755	80.458	79.934	66.096	Improved Rangeland
(36)	834	83.080	40.642	151.531	Winter Wheat - Spring and Fall
(37)	4290	83.953	65.860	43.336	Woodland
(38)	1607	90.225	101.694	45.889	Woodland
(39)	1827	91.781	38.296	104.199	Winter Wheat - Spring and Fall
(40)	2225	92.042	56.407	76.644	Winter Wheat - Spring and Fall
(41)	3130	93.760	80.818	42.382	Woodland
(42)	2146	97.782	45.846	50.539	Winter Wheat - Spring Only
(43)	2133	102.429	29.022	69.386	Winter Wheat - Spring and Fall
(44)	755	102.620	79.054	105.110	Spring, Summer, and Fall Crops
(45)	804	117.279	69.531	69.270	Winter Wheat - Spring Only
(46)	1675	119.487	30.361	32.936	Winter Wheat - Spring Only
(47)	689	120.055	36.322	136.737	Winter Wheat - Spring and Fall
(48)	1292	123.720	34.063	96.144	Winter Wheat - Spring and Fall
(49)	1364	129.013	28.614	63.247	Winter Wheat - Spring and Fall
(50)	323	151.025	119.375	101.613	Spring, Summer, and Fall Crops

TABLE VII
CLUSTER SIGNATURE LISTING FOR 1986

Cluster	Count	Spring	Summer	Fall	Class
(1)	58659	0.023	0.019	0.012	Water, Urban, Bare
(2)	322	6.926	10.432	39.761	Water, Urban, Bare
(3)	278	8.191	74.237	49.863	Water, Urban, Bare
(4)	470	28.438	58.202	12.730	Native Rangeland
(5)	2182	42.843	45.056	36.122	Water, Urban, Bare
(6)	4204	44.675	67.577	33.043	Native Rangeland
(7)	387	46.773	25.279	64.354	Native Rangeland
(8)	4438	46.845	60.727	49.208	Native Rangeland
(9)	4423	50.775	80.569	52.036	Summer Crops
(10)	258	52.671	10.240	8.601	Water, Urban, Bare
(11)	3063	52.718	69.005	71.442	Woodland
(12)	4047	52.457	82.491	34.441	Improved Rangeland
(13)	4800	52.703	56.593	33.462	Native Rangeland
(14)	7826	56.293	69.692	40.570	Woodland
(15)	2297	56.112	104.316	45.401	Improved Rangeland
(16)	1920	57.010	46.092	56.730	Native Rangeland
(17)	1957	59.000	96.188	74.831	Summer and Fall Crops
(18)	5735	61.064	65.692	54.895	Native Rangeland
(19)	5144	62.695	57.235	42.682	Native Rangeland
(20)	1239	63.519	37.866	95.234	Winter Wheat - Fall Only
(21)	449	64.200	2.711	45.040	Water, Urban, Bare
(22)	4564	65.431	67.298	29.804	Native Rangeland
(23)	5078	65.925	83.052	55.064	Native Rangeland
(24)	5620	67.396	83.250	36.778	Woodland
(25)	6699	69.308	71.554	43.969	Improved Rangeland
(26)	2328	69.260	72.972	86.480	Improved Rangeland
(27)	1173	72.637	68.962	122.113	Winter Wheat - Fall Only
(28)	2328	72.398	54.601	68.615	Winter Wheat - Spring Only
(29)	1402	74.014	34.814	40.611	Improved Rangeland
(30)	4296	75.754	70.634	60.144	Improved Rangeland
(31)	2697	78.423	98.839	44.560	Summer Crops
(32)	1484	78.875	120.226	65.729	Summer Crops
(33)	3185	81.967	58.463	43.817	Winter Wheat - Spring Only
(34)	3067	82.293	87.147	66.063	Spring and Summer Crops
(35)	1365	84.163	32.292	74.309	Winter Wheat - Spring and Fall
(36)	3948	85.088	77.632	40.456	Woodland
(37)	1521	88.139	33.038	114.168	Winter Wheat - Spring and Fall
(38)	761	88.838	35.594	153.376	Winter Wheat - Spring and Fall
(39)	1399	90.646	58.668	92.400	Winter Wheat - Spring and Fall
(40)	1394	94.123	97.546	88.852	Spring, Summer, and Fall Crops
(41)	2509	100.408	66.564	62.954	Winter Wheat - Spring and Fall
(42)	1450	102.899	34.717	54.070	Winter Wheat - Spring Only
(43)	1639	104.633	92.941	53.344	Spring and Summer Crops
(44)	1014	110.318	42.181	31.782	Winter Wheat - Spring Only
(45)	1574	114.867	33.782	85.987	Winter Wheat - Spring and Fall
(46)	693	124.522	73.937	102.515	Winter Wheat - Spring and Fall
(47)	1059	124.250	33.705	117.502	Winter Wheat - Spring and Fall
(48)	1047	136.294	32.974	51.204	Winter Wheat - Spring Only
(49)	888	135.749	72.096	56.788	Winter Wheat - Spring Only
(50)	481	146.168	113.391	77.081	Spring and Summer Crops

TABLE VIII
CLUSTER SIGNATURE LISTING FOR 1988

Cluster	Count	Spring	Summer	Fall	Class
(1)	58970	0.024	0.016	0.010	Water, Urban, Bare
(2)	379	4.855	62.496	54.385	Water, Urban, Bare
(3)	367	7.826	42.063	27.542	Water, Urban, Bare
(4)	645	38.459	25.236	26.465	Water, Urban, Bare
(5)	1940	42.128	41.072	56.830	Native Rangeland
(6)	1269	42.907	84.597	43.101	Summer Crops
(7)	3330	43.870	40.969	34.453	Native Rangeland
(8)	1518	49.192	69.681	81.615	Summer and Fall Crops
(9)	3798	50.352	61.988	45.690	Native Rangeland
(10)	1032	51.533	31.373	166.371	Winter Wheat - Fall Only
(11)	4424	52.237	52.905	29.363	Native Rangeland
(12)	317	54.886	2.896	3.514	Water, Urban, Bare
(13)	3790	56.928	35.511	31.763	Native Rangeland
(14)	2149	56.419	33.383	96.572	Winter Wheat - Fall Only
(15)	6262	57.589	46.173	43.358	Native Rangeland
(16)	3417	58.222	30.824	49.862	Native Rangeland
(17)	4424	59.563	49.993	60.475	Native Rangeland
(18)	1071	61.103	110.275	51.312	Summer Crops
(19)	3113	62.555	81.244	38.484	Woodland
(20)	3644	62.532	35.248	73.047	Native Rangeland
(21)	3966	65.241	63.147	34.758	Native Rangeland
(22)	4275	65.347	66.933	59.299	Native Rangeland
(23)	1977	65.718	33.812	128.579	Winter Wheat - Fall Only
(24)	1501	68.051	65.484	109.295	Winter Wheat - Fall Only
(25)	420	71.481	137.460	116.512	Summer and Fall Crops
(26)	2809	68.778	85.652	58.822	Woodland
(27)	588	67.427	67.791	143.541	Summer and Fall Crops
(28)	4674	69.442	44.958	33.667	Native Rangeland
(29)	5451	70.365	54.326	47.032	Improved Rangeland
(30)	3553	71.978	57.158	80.001	Improved Rangeland
(31)	4560	72.037	38.657	53.348	Improved Rangeland
(32)	1859	78.561	87.954	82.839	Spring, Summer, and Fall Crops
(33)	4278	79.892	68.710	43.654	Woodland
(34)	2092	80.615	37.033	98.593	Winter Wheat - Spring and Fall
(35)	4259	81.423	49.715	62.077	Improved Rangeland
(36)	2156	81.370	25.814	40.755	Winter Wheat - Spring Only
(37)	218	84.858	4.005	3.509	Winter Wheat - Spring Only
(38)	2596	84.740	30.371	75.256	Winter Wheat - Spring and Fall
(39)	3186	85.862	87.539	44.286	Woodland
(40)	673	86.746	36.915	161.909	Winter Wheat - Spring and Fall
(41)	3335	87.566	69.457	62.101	Improved Rangeland
(42)	3825	87.880	49.291	39.184	Winter Wheat - Spring Only
(43)	2162	98.357	58.492	82.791	Winter Wheat - Spring and Fall
(44)	974	100.580	42.501	120.961	Winter Wheat - Spring and Fall
(45)	1181	102.436	104.627	50.699	Woodland
(46)	2716	103.377	64.165	45.390	Woodland
(47)	2075	105.968	39.258	53.548	Winter Wheat - Spring Only
(48)	2717	106.128	84.177	55.254	Woodland
(49)	756	105.950	88.058	109.323	Spring, Summer, and Fall Crops
(50)	413	139.269	63.707	77.041	Spring, Summer, and Fall Crops

of pasture grass which was irrigated or fertilized. Those classes representing agricultural crops had less vague growth patterns, as an agricultural field would either show a very high or very low greenness value, depending on whether a crop was planted or not. These classes appeared as bright colors in the image due to the color combinations resulting from the growth patterns, whereas non-agricultural classes had greenness values in the low to middle range in their signatures. Areas representing water, bare soil, or urban cover were also easily identified as having little or no growth in all seasons. A more specific description of the average signature statistics will be given below.

Spatial image interpretation techniques were also used to assign each cluster to the appropriate land cover class. Those clusters representing agricultural crops were easily identified because they usually contained many contiguous pixels that represented a field planted with the same crop in the same growth state. However, the signatures for rangelands and woodlands were sometimes similar. For this reason, a familiarity with the spatial patterns of the watershed was necessary to identify areas with known land cover that did not change from year to year. Large tree stands, riparian zones, and dominant rangelands were identified on aerial photographs and were located on the source image. This information was helpful but was not used exclusively to determine land cover for those areas.

When all clusters were classified, the spectral signatures were merged according to each land cover class. When merged, the average signatures were found for each class, and were then examined in order to analyze class separability and to compare to signatures for the other years. Tables XIII-XVI list the classes' average signatures for each year. The final average land cover class signatures show that each class had

essentially the same greenness pattern for the three acquisition dates, but the signature averages were not the same for every class from year to year. These variations can be attributed to varying dates of acquisition for each point in the growing season for each year and wide spectral ranges due to mixed pixels.

The most major discrepancy between yearly averages occurred in the Woodland class in 1976, in the fall of that year. The fall signature value in that class was much higher (56.729) than the other three years' (42.181 in 1984, 47.312 in 1986, and 48.084 in 1988). The date of the fall scene used in 1976 was 13 October, which was the earliest fall image of the four years. The other three were 10 November 1984, 31 October 1986, and 5 November 1988. The time difference should not account for the 1976 result, but could be attributed to a late senescence of woodland vegetation in that year. The woodland classes were identified by the existence of known tree stands as shown on

TABLE IX
AVERAGE SPECTRAL SIGNATURE STATISTICS
FOR 1976

Class name	Spring	Summer	Fall
Water, Urban, Bare Soil	0.054	0.034	0.052
Native Rangeland	21.624	22.310	27.176
Improved Rangeland	34.547	45.945	43.928
Woodland	44.603	64.868	56.729
Winter Wheat - Spring Only	66.741	10.472	21.161
Winter Wheat - Fall Only	14.657	8.458	76.844
Winter Wheat - Spring and Fall	69.530	10.288	64.055
Summer Crops	15.489	104.862	26.049
Spring & Summer Crops	115.274	121.425	49.321
Summer & Fall Crops	18.312	114.539	66.212
Spring, Summer, & Fall Crops	90.003	110.285	104.914

TABLE X
AVERAGE SPECTRAL SIGNATURE STATISTICS
FOR 1984

Class name	Spring	Summer	Fall
Water, Urban, Bare Soil	16.239	28.914	25.039
Native Rangeland	54.645	50.939	38.675
Improved Rangeland	68.099	61.507	61.956
Woodland	74.882	77.961	42.181
Winter Wheat - Spring Only	103.450	46.803	47.060
Winter Wheat - Fall Only	44.304	29.562	104.130
Winter Wheat - Spring and Fall	96.664	39.919	95.822
Summer Crops	63.599	114.043	67.263
Spring & Summer Crops	NA	NA	NA
Summer & Fall Crops	68.557	142.882	120.841
Spring, Summer, & Fall Crops	126.822	99.214	103.362

TABLE XI
AVERAGE SPECTRAL SIGNATURE STATISTICS
FOR 1986

Class name	Spring	Summer	Fall
Water, Urban, Bare Soil	29.142	23.783	29.900
Native Rangeland	53.156	58.775	43.197
Improved Rangeland	66.151	72.797	51.841
Woodland	65.374	74.895	47.312
Winter Wheat - Spring Only	106.604	49.172	51.046
Winter Wheat - Fall Only	68.078	53.414	108.674
Winter Wheat - Spring and Fall	101.979	45.948	100.402
Summer Crops	69.358	99.878	54.108
Spring & Summer Crops	111.031	97.826	65.496
Summer & Fall Crops	59.000	96.188	74.831
Spring, Summer, & Fall Crops	94.123	97.546	88.852

TABLE XII
AVERAGE SPECTRAL SIGNATURE STATISTICS
FOR 1988

Class name	Spring	Summer	Fall
Water, Urban, Bare Soil	21.210	26.541	22.383
Native Rangeland	56.954	47.477	46.047
Improved Rangeland	76.674	53.862	60.912
Woodland	87.004	82.302	48.084
Winter Wheat - Spring Only	90.019	29.592	34.249
Winter Wheat - Fall Only	60.430	41.013	125.205
Winter Wheat - Spring and Fall	90.208	41.062	107.902
Summer Crops	52.005	97.436	47.206
Spring & Summer Crops	NA	NA	NA
Summer & Fall Crops	62.700	91.644	113.889
Spring, Summer, & Fall Crops	107.927	79.906	89.734

aerial photographs and image interpretation. These techniques were reliable for this classification in spite of the inconsistency of the growth patterns for trees in 1976 in comparison with other years.

It is important to note that these signatures are the means of the ranges of the original cluster signatures. The minimum and maximum greenness values in each cluster were affected by class mixing, where one pixel may have contained more than one cover type. In such a situation, the dominant cover type was determined by the multitemporal growth pattern, but would result in varying signature statistics. An example of this can be seen in the lower ranges of Class 31 in the 1976 image which was classified as Winter Wheat - Spring Only based on its growth pattern, in addition to the relative locations of the pixels in that cluster which were adjacent to large wheat fields. The greenness value in the spring for Class 31 was a low 43.678, but the extremely low values in the summer

and fall (1.552 and 10.575) indicate the appropriate growth pattern of the class that cluster was assigned to. This signature, when averaged with the other five Winter Wheat - Spring Only clusters, contributed to the lower average spring signature (66.741) in comparison with the other years' (103.450, 106.604, and 90.019).

Every class except Woodland in 1976 exhibited very similar signature statistics and growth patterns in each year. However, the Spring and Summer Crops class was not used in every years' classifications as no clusters were found that met the criteria for that class in two of the years studied. Crops grown in both spring and summer but not fall were only found in 1976 and 1986.

The class signatures for each of the four years were averaged in order to develop a general multitemporal spectral profile for the Little Washita Watershed. Table XVII lists the combined average signatures for all four years. This information can be used to

TABLE XIII
COMBINED AVERAGE SPECTRAL SIGNATURE STATISTICS
FOR 1976, 1984, 1986, AND 1988

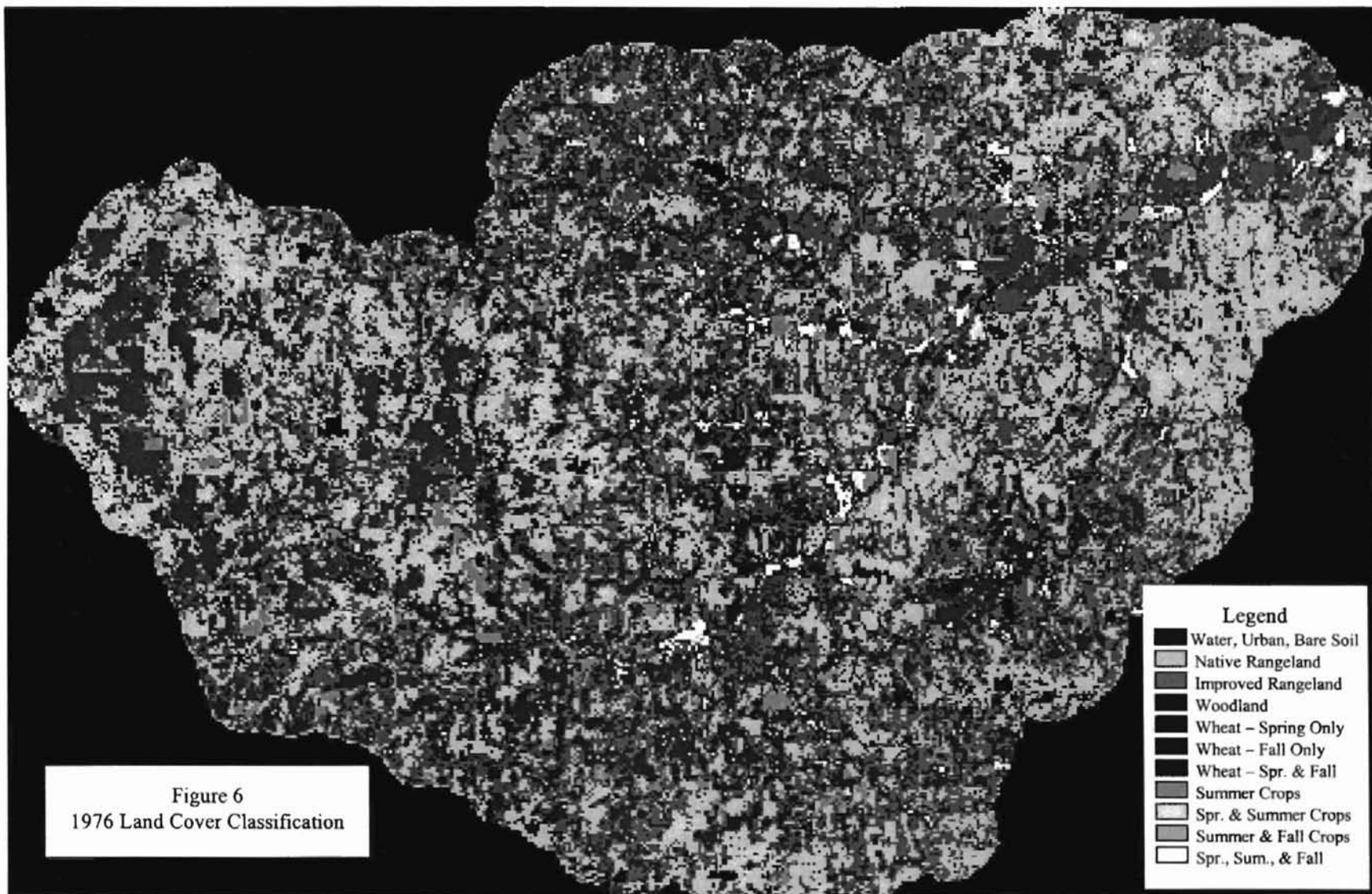
Class name	Spring	Summer	Fall
Water, Urban, Bare Soil	16.661	19.818	19.344
Native Rangeland	46.595	44.875	38.774
Improved Rangeland	61.367	58.528	54.659
Woodland	67.966	75.007	48.576
Winter Wheat - Spring Only	91.703	34.010	38.379
Winter Wheat - Fall Only	46.867	33.112	103.713
Winter Wheat - Spring and Fall	89.595	34.304	92.045
Summer Crops	50.113	104.055	48.657
Spring & Summer Crops*	113.152	109.626	57.408
Summer & Fall Crops	52.142	111.313	93.943
Spring, Summer, & Fall Crops	104.719	96.738	96.716

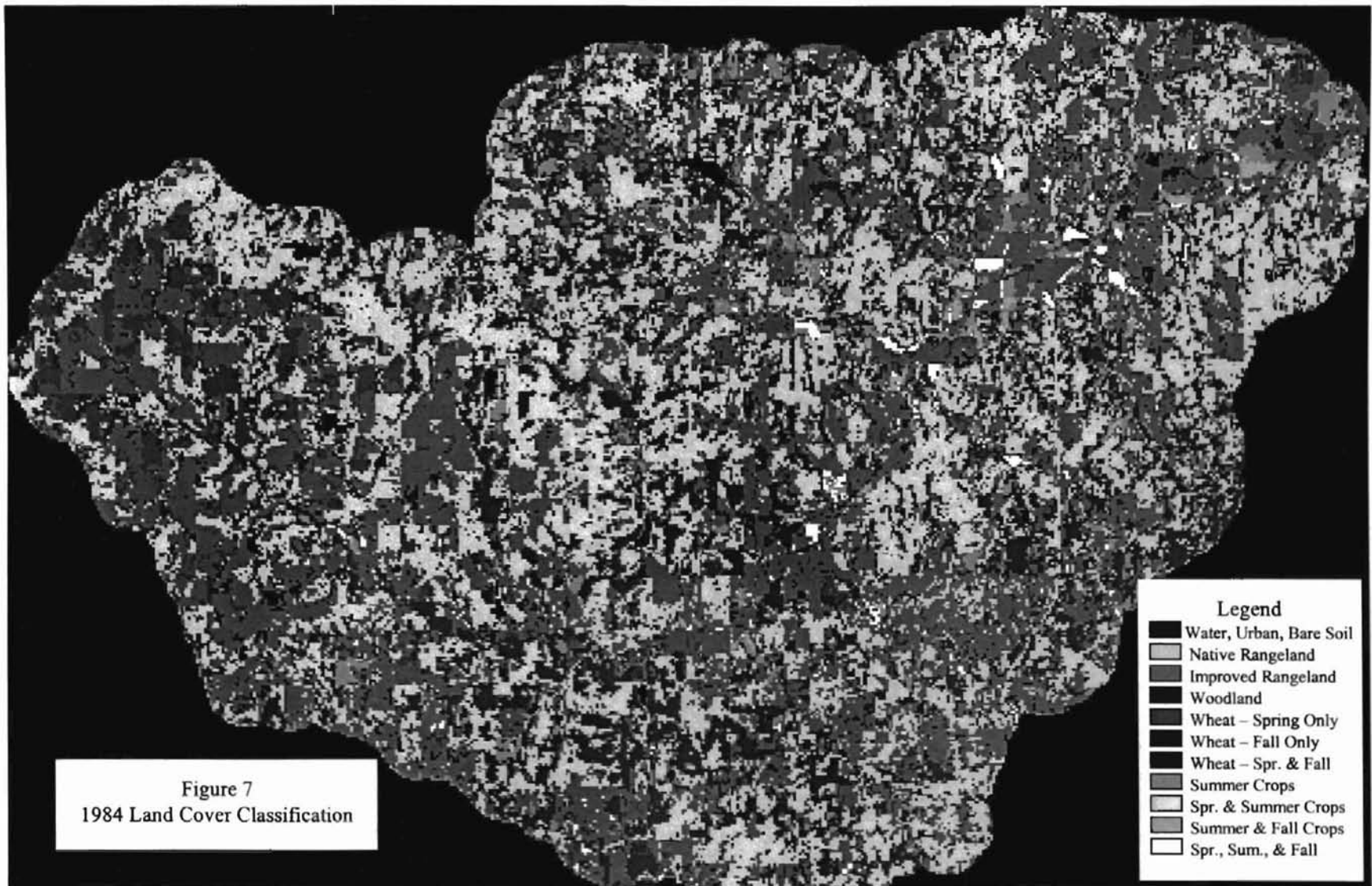
*1976 and 1986 only

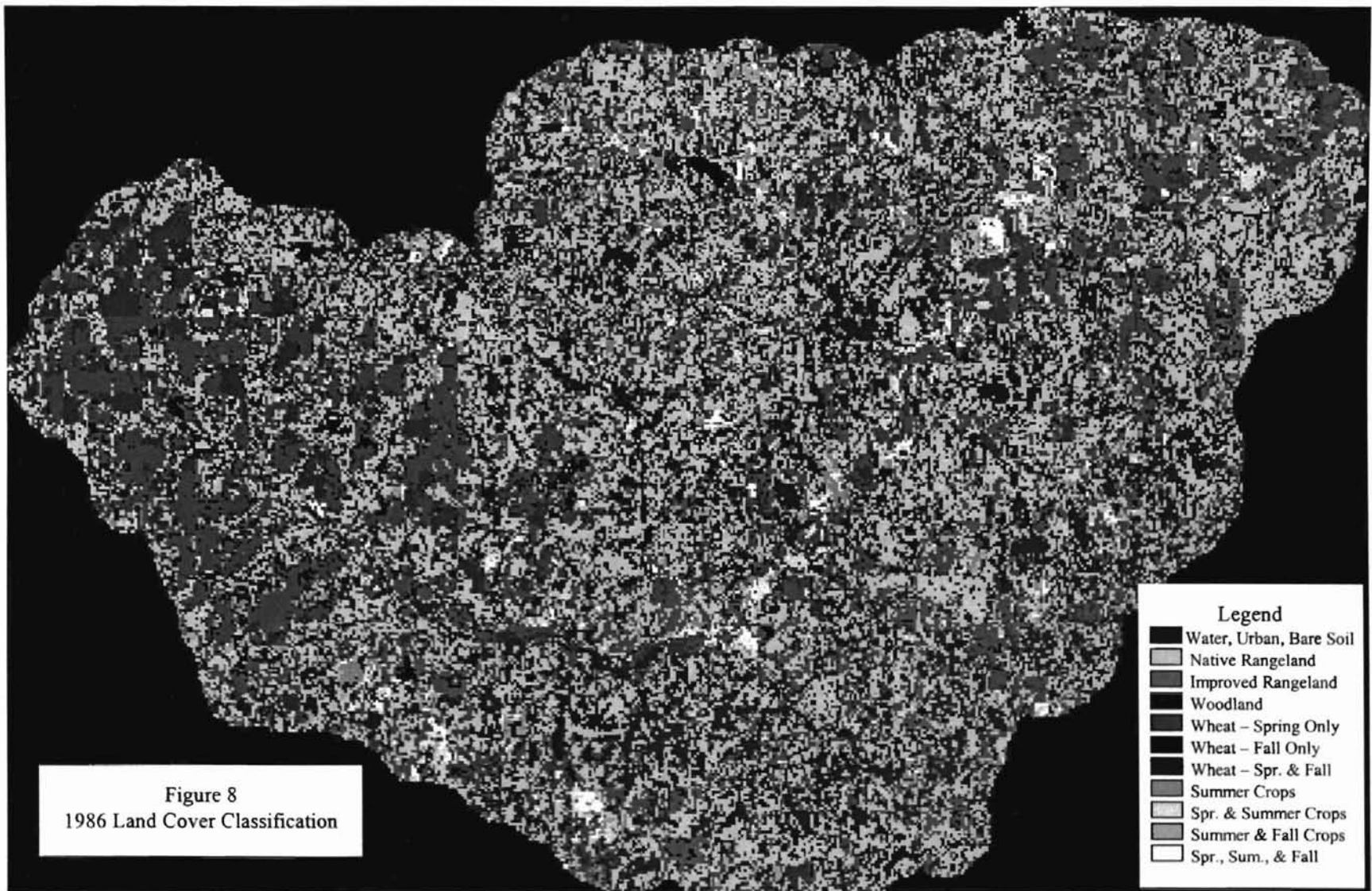
quickly classify the other multitemporal images that will be generated for the Little Washita project. It is possible for classification algorithms to use a pre-defined signature file and assign each pixel directly to a land cover class, bypassing the interpretation of a forty-cluster output image. However, more conclusive data concerning the incomplete classes for every year should be derived for a reliable classification using this method.

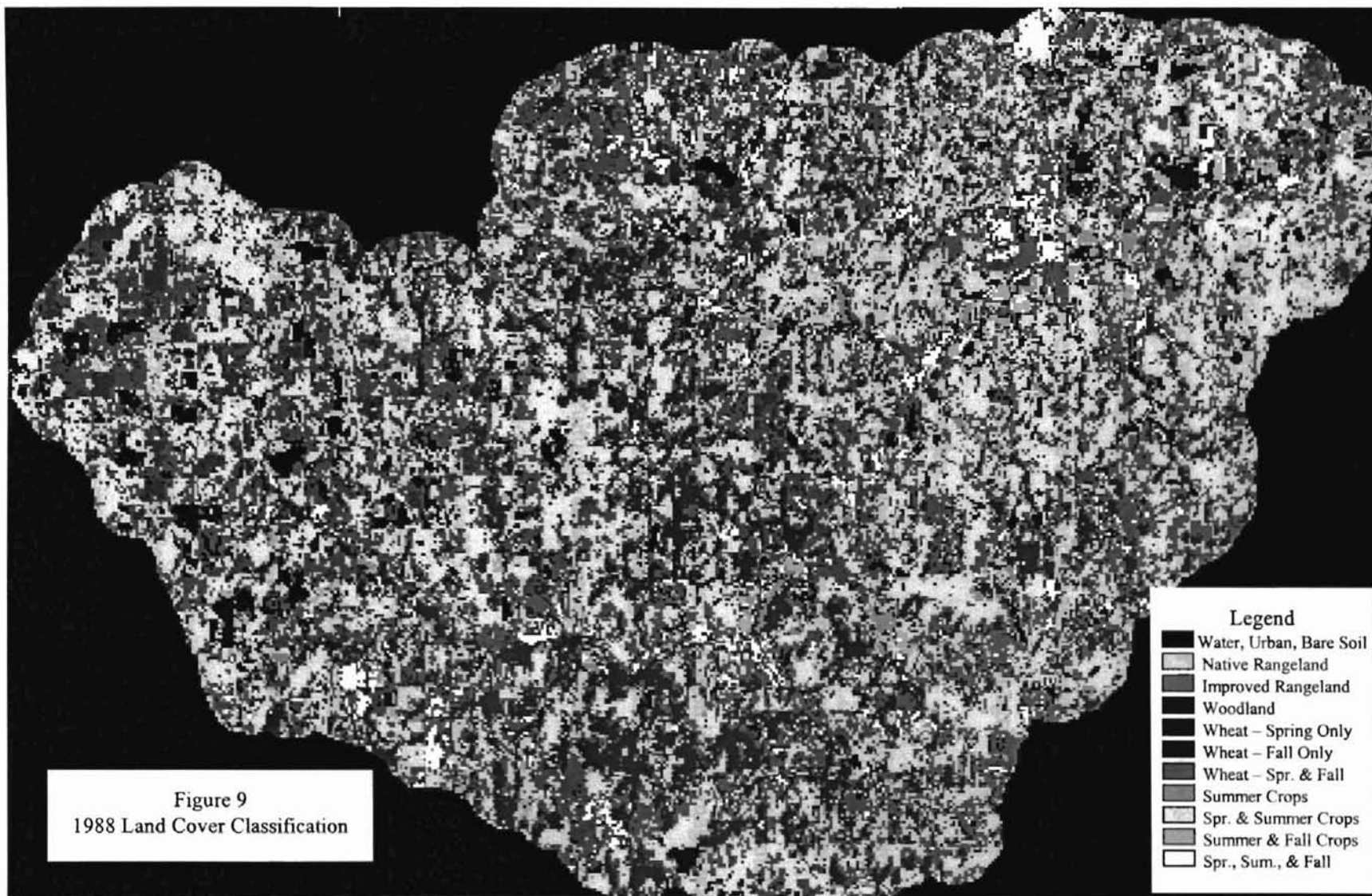
Classification Results for Each Year

The final output of the classification process consisted of the eleven-class image described above. The land cover maps for each year are shown in Figures 6-9. As mentioned earlier, there is no way to test the accuracy of these classifications without field verification data. However, the unique multitemporal spectral profiles of the classes and their consistency from year to year were reliable indicators of general cover types, especially when dealing with agricultural crops due to their homogeneous nature both in spatial and spectral terms (Lo et al., 1986). The non-agricultural Woodland and Rangeland classes were somewhat more difficult to separate from each other when their growth patterns were similar. This problem was encountered in the 1986 classification where some clusters contained pixels in areas which were known to have both wooded and rangeland covers, but were assigned to the same cluster. The spectral response for Improved Rangeland was very close to that of Woodland in this image, and resulted in pixels which were classified as Woodland that appeared in areas that were known to be Rangeland. The effect of this problem can be seen in the map of the 1986 classification in Figure 8, where pixels assigned to the Improved Rangeland and Woodland classes









were mixed significantly.

In the absence of any information regarding the locations of the two types of rangeland used in this study, the only criteria used to differentiate the two was the greenness spectral response, which was assumed to be higher for improved rangelands. These problems accounted for the discrepancies between non-agricultural cover types as they appear on the maps. However, it can be said that the agricultural classes were differentiated between crop types and were distinguished from non-agricultural classes successfully with the method developed in this study.

The numbers of pixels assigned to each class in each year's classification are listed in Tables XVIII-XXI. Also listed are the total acres represented by each class. The number of acres covered by one MSS pixel is 1.6 (Avery and Berlin, 1992). The total number of acres delineated by the 500 meter buffer boundary polygon in the images was 198897.6. Various assessments may be made by comparing acre counts for different cover types between years, such as agricultural versus non-agricultural land or the amount of land used specifically for growing winter wheat. For example, the number of acres found to have an agricultural land cover in 1986 (64555.2 ac.) was significantly greater than in the other three years (45430.4 ac. in 1976, 45204.8 ac. in 1984, and 50118.4 ac in 1988). This appeared to be abnormal until the agricultural land cover counts were examined for those areas classified as growing either winter wheat or crops grown in summer.

Table XIX shows the number of acres belonging to the following groups of classes: Non-Crop (Water/Urban/Bare Soil, Native Rangeland, Improved Rangeland), and Agricultural (all other classes). The other two groups were selected from the Crops

TABLE XIV
CLASS PIXEL COUNTS
FOR 1976

Class name	Count	Acres
Water, Urban, Bare Soil	3098	4956.8
Native Rangeland	30647	49035.2
Improved Rangeland	30821	49313.6
Woodland	31351	50161.6
Winter Wheat - Spring Only	4607	7371.2
Winter Wheat - Fall Only	3972	6355.2
Winter Wheat - Spring and Fall	2380	3665.2
Summer Crops	6131	9809.6
Spring & Summer Crops	280	448.0
Summer & Fall Crops	6712	10739.2
Spring, Summer, & Fall Crops	4312	6899.2

TABLE XV
CLASS PIXEL COUNTS
FOR 1984

Class name	Count	Acres
Water, Urban, Bare Soil	4616	7385.6
Native Rangeland	38004	60806.4
Improved Rangeland	27301	43681.6
Woodland	26137	41819.2
Winter Wheat - Spring Only	6667	10667.2
Winter Wheat - Fall Only	1420	2272.0
Winter Wheat - Spring and Fall	15318	24508.8
Summer Crops	3373	5396.8
Spring & Summer Crops	NA	NA
Summer & Fall Crops	397	635.2
Spring, Summer, & Fall Crops	1078	1724.8

TABLE XVI
CLASS PIXEL COUNTS
FOR 1986

Class name	Count	Acres
Water, Urban, Bare Soil	5698	9116.8
Native Rangeland	36740	58784.0
Improved Rangeland	21069	33710.4
Woodland	20457	32731.2
Winter Wheat - Spring Only	9912	15859.2
Winter Wheat - Fall Only	2412	3859.2
Winter Wheat - Spring and Fall	10881	17409.6
Summer Crops	8604	13766.4
Spring & Summer Crops	5187	8299.2
Summer & Fall Crops	1957	3131.2
Spring, Summer, & Fall Crops	1394	2230.4

TABLE XVII
CLASS PIXEL COUNTS
FOR 1988

Class name	Count	Acres
Water, Urban, Bare Soil	4228	6764.8
Native Rangeland	47944	76710.4
Improved Rangeland	21158	33852.8
Woodland	20000	32000.0
Winter Wheat - Spring Only	8274	13238.4
Winter Wheat - Fall Only	6659	10654.4
Winter Wheat - Spring and Fall	8497	13595.2
Summer Crops	2340	3744.0
Spring & Summer Crops	NA	NA
Summer & Fall Crops	2526	4041.6
Spring, Summer, & Fall Crops	3028	4844.8

group: Winter Wheat (Spring Only, Fall Only, Spring and Fall), and All Summer Crops (Summer Crops, Spring and Summer, Summer and Fall, and Spring, Summer and Fall). In 1976, only 17534.4 acres were estimated to be used to grow winter wheat, compared to 37448.0 acres in 1984, 37128.0 in 1986, and 37488.0 in 1988. Classes that included all crops grown in summer in 1986 totaled 27427.2 acres, which was close to the 27896.0 acres estimated for 1976. 1984 and 1988 had only 7756.8 and 12630.4 acres in summer crops, respectively. So, the larger number of agricultural land cover acres in 1986 may be explained by the estimates for both the winter wheat and summer crop classes, which were both high compared to the other three years.

TABLE XVIII
ACRES IN SELECTED CLASS GROUPS

Year	Non-Crop	Crops	Winter Wheat	All Summer Crops
1976	153467.2	45430.4	17534.4	27896.0
1984	153692.8	45204.8	37448.0	7756.8
1986	134342.4	64555.2	37128.0	27427.2
1988	149328.0	50118.4	37488.0	12630.4

Another discrepancy may be found when comparing the counts for the Woodland class. It may be assumed that the amount of land covered by trees in the Little Washita watershed would not have changed as significantly as is indicated by the classifications created in this study. The number of acres classified as Woodlands in 1976 was 50161.6, 41819.2 acres in 1984, 32731.2 in 1986, and 32000.0 in 1988. While it is expected for woodlands to be cleared for agricultural use or rangeland, it is doubtful that almost 20000 acres of woodland were cleared between 1976 and 1988 for this purpose. This error was

attributed to the relative inability of the classification method to discern between woodland and rangeland signatures, as described above.

CHAPTER FIVE

CONCLUSIONS

Summary

The purpose, objective, and method of the derivation of a land cover classification using multitemporal Landsat MSS data has been described. The National Agricultural Water Quality Laboratory has undertaken a time-series hydrologic study of the Little Washita Watershed for which land cover data is needed, especially that of crop cover inventory. Land cover information for every even-numbered year from 1972 to 1992 will be derived from a data set that consists of three MSS scenes from each of those years. This study has examined the creation of a procedure which produced multitemporal land cover classifications for four of those years: 1976, 1984, 1986, and 1988.

The main objective of this study was to use the three scenes from each year to represent distinct points in a growing season: spring, summer, and fall, and derive a classification from those images which could distinguish crop types by their presence at those times in the growing season. It is generally accepted that land cover classifications generated from a single date are not comprehensive, especially when attempting to identify different types of agricultural land covers (Lo et al., 1986). The alternative method that was used was to compress the multispectral data and combine images from different dates. Several techniques for reducing the dimensionality and redundancy of multispectral imagery were reviewed, including the normalized difference vegetation

index, principal components analysis, and the Kauth-Thomas Tasseled Cap transformation. The Tasseled Cap was used to reduce a four-band MSS scene into a one-band Greenness Vegetation Index. The vegetation indices derived from the spring, summer, and fall scenes from one year were combined as a three-band image, which was then classified using an unsupervised method. Land cover classes were determined using conventional image interpretation techniques and the use of multitemporal spectral profiles based on the growth patterns of different cover types at the three points in the growing season. Multitemporal land cover maps were created which identified the types of crops that were grown and at which points in the growing season crops were present in addition to rangelands, woodland, and non-vegetative land covers.

Discussion of Research Findings

The land cover maps derived from the multitemporal MSS imagery in this study are unique representations of the Little Washita Watershed landscape, especially concerning agricultural change detection. While there are discrepancies involving the accuracy of such classifications due to the lack of field verification information, the methods developed in this study and the derivation of specific vegetation profiles for the Little Washita area are valuable for continuing research.

Several previous studies have used multitemporal imagery for the detection of land cover change, but the specific objectives and methodology used for this research were unique. The overlay and false-color composite of three vegetation indices provided an easy and informative means of observing land cover change through a growing season.

Also, the general spectral signatures that were derived from the four years used in this study will be used in future classifications for the Little Washita research. The signatures resulting from the agricultural classes were definitive and consistent for each of the four years. The variations in classification of the rangeland and wooded areas reveal limitations in the process, but the growth patterns of these cover types should become more defined as more years' classifications are processed. A standard set of signatures should increase the reliability of the non-agricultural class assignments.

The analysis of the findings in this study show that the use of multitemporal remotely sensed data to identify agricultural land cover without the aid of field verification data can be performed effectively using the methods described. The Kauth-Thomas Greenness Vegetation Index has been shown to be a very useful tool for extracting important vegetation information from multispectral data and for the derivation of spectral profiles which are indicative of different land cover types. The Tasseled Cap transformation was developed for agricultural observation and is most effective when applied to that end. The land cover information needed for the hydrologic research in the Little Washita Watershed is focused primarily on crop cover inventory and the results of this study have provided a valuable means of detecting agricultural land cover change.

Recommendations for Future Research

The most important factor in the continuing research for this project is the use of better data sources. The need for multispectral data for the earliest dates possible predetermined the use of MSS, but the accuracy of this method would be greatly

increased with the use of higher quality imagery. Thematic Mapper scenes have been acquired for the study of the Little Washita Watershed for three points in the 1994 growing season. Using field verification data gathered for all three dates, the multitemporal classification of the TM imagery would be able to be measured for accuracy, and would result in a more effective set of spectral profiles, particularly for the non-agricultural classes. As subsequent sensor platforms continue to be launched, the availability of better data sources increases, as does the accuracy of derived land cover classifications.

The other transformation techniques reviewed in this study should also be applied and investigated for their effectiveness. The underlying concept of and the output from principal components analysis are often confusing, but PCA has been shown to extract valuable information that differs from those producing vegetation indices. Other transformations such as canonical analysis and Leaf Area Index may also be investigated for use in multitemporal land cover studies. Different spectral profiles may be developed in combination with vegetation information that could further separate those cover types with similar signatures. Incorporating this kind of information and using the methods described in this study enables the use of historical remote sensing data to detect land cover change without the aid of field verification data.

BIBLIOGRAPHY

Allen, Paul B. and James W. Naney. 1991. Hydrology of the Little Washita Watershed, Oklahoma. Durant OK: USDA - Agricultural Research Service

Anderson, James R., Ernest. E. Hardy, John. T. Roach, and Richard. E. Witmer. 1976. A Land Use and Land Cover Classification System for Use with Remote Sensor Data. Geologic Survey Paper 964. Washington, D.C.: U.S. Government Printing Office.

Avery, Thomas E., G. L. Berlin. 1992. Fundamentals of Remote Sensing and Airphoto Interpretation (5th ed.). New York: Macmillan Publishing Company.

Badhwar, Gautam D., and Keith E. Henderson. 1985. Application of Thematic Mapper data to corn and soybean development stage estimation. Remote Sensing of Environment. Vol. 17: 197-201.

Byrne, G. F., P. F. Crapper, and K. K. Mayo. 1980. Monitoring land-cover change by principle component analysis of multitemporal Landsat data. Remote Sensing of Environment. Vol. 10: 175-184.

Crist, E.P. and R.J. Kauth. 1986. The Tasseled Cap De-Mystified. Photogrammetric Engineering and Remote Sensing. Jan. 1986: 81-86.

Engvall, John L., J.D. Tubbs, and Q.A. Holmes. 1977. Pattern recognition of Landsat data based upon trend analysis. Remote Sensing of Environment. Vol. 6: 1-13.

Fischer, A. 1994. A model for the seasonal variations of vegetation indices in coarse resolution data and its inversion to extract crop parameters. Remote Sensing of Environment. Vol. 48: 220-230.

Fostel, Henry F., James E. Manley, and James P. Ormsby. 1979. The use of Landsat multispectral data to derive land cover information for the location and quantification of non-point source water pollutants. Purdue: LARS Symposium on Machine Processing of Remotely Sensed Data. IEEE Catalog Number CH1430, 1979.

Gammon, Patricia T. and Virginia P. Carter. 1976. Comparison of vegetation classes in the Great Dismal Swamp using two individual Landsat images and a temporal composite. Purdue: LARS Symposium on Machine Processing of Remotely Sensed Data. IEEE Catalog Number CH1103-IMPRSD, 1976.

Gordon, Steven I. 1980. Utilizing Landsat imagery to monitor land-use change: a case study in Ohio. *Remote Sensing of Environment*. Vol. 9: 189-196.

Hlavka, Christine A., S. M. Carlyle, R. Yokoyama, and R. M. Haralick. 1979. Multi-temporal classification of winter wheat using a growth state model. Purdue: LARS Symposium on Machine Processing of Remotely Sensed Data. IEEE Catalog Number 79CH1430-8MPRSD, 1979.

Holben, B. N. 1986. Characteristics of maximum-value composite images from temporal AVHRR data. *International Journal of Remote Sensing*. Vol. 7, no. 11: 1417-1434.

Hord, Michael R. 1986. *Remote Sensing*. New York: John Wiley & Sons.

Howarth, Philip J. and Emil Boasson. 1983. Landsat digital enhancements for change detection in urban environments. *Remote Sensing of Environment*. Vol. 13: 149-160.

Iqbal, M. 1983. *An Introduction to Solar Radiation*. New York: Academic Press.

Jackson, T.J. and F.R. Schiebe. 1992. *Hydrology Data Report - Washita '92*. Durant, OK: USDA - Agricultural Research Center.

Kaneko, Toyohisa. 1978. Crop classification using time features computed from multi-temporal multi-spectral data. *Proceedings: 1978 Conference on Pattern Recognition and Image Processing*. New York:IEEE, 1978.

Kauth, R. J. and G. S. Thomas. 1976. *The Tasseled Cap - A graphic description of the spectral-temporal development of agricultural crops as seen by LANDSAT*. Environmental Research Institute of Michigan. Ann Arbor, MI.

Lillesand, Thomas M. and Ralph W. Kiefer. 1994. *Remote Sensing and Image Interpretation (3rd ed.)*. New York: John Wiley & Sons.

Lambin, E. F., and A. H. Strahler. 1994. Change-vector analysis in multitemporal space: a tool to detect and categorize land-cover change processes using high temporal-resolution satellite data. *Remote Sensing of Environment*. Vol. 48: 231-244.

Lo, Thomas H. C., F. L. Scarpace, and T. M. Lillesand. 1986. Use of multitemporal spectral profiles in agricultural land-cover classification. *Photogrammetric Engineering and Remote Sensing*. Vol. 52, no. 4: 535-544.

Lucas, R.M., M. Honzak, G. M. Foody, P. J. Curran, and C. Corves. 1993. Characterizing tropical secondary forests using multi-temporal Landsat sensor imagery. *International Journal of Remote Sensing*. Vol. 14, no. 16: 3061-3067.

Markham, B. L., and J. L. Barker. 1986. Landsat MSS and TM post-calibration dynamic ranges, exoatmospheric reflectances and at-satellite temperatures. *EOSAT Technical Notes*. v. 1: 3-8.

Price, John C. 1987. Calibration of satellite radiometers and the comparison of vegetation indices. *Remote Sensing of Environment*. Vol. 21:15-27.

Richardson, A. J., and C. L. Wiegand. 1977. Distinguishing vegetation from soil background information. *Photogrammetric Engineering and Remote Sensing*. Vol. 43, no. 12: 1541-1552.

Samson, Scott A. 1993. Two indices to characterize temporal patterns in the spectral response of vegetation. *Photogrammetric Engineering and Remote Sensing*. Vol. 59, no. 4: 511-517.

Schiebe, F. R., J. A. Harrington, Jr. and J. C. Ritchie. 1992. Remote sensing of suspended sediments: the Lake Chicot, Arkansas project. *International Journal of Remote Sensing*. Vol. 13, no. 8: 1487-1509.

Singh, Ashbindu. 1989. Digital change detection techniques using remotely-sensed data. *International Journal of Remote Sensing*. Vol. 10, no. 6: 989-1003.

VITA

Christopher G. Berry

Candidate for the Degree of

Master of Science

THESIS: MULTITEMPORAL LAND COVER CLASSIFICATION OF THE
LITTLE WASHITA WATERSHED USING THE KAUTH-THOMAS
GREENNESS VEGETATION INDEX

Major Field: Geography

Biographical:

Personal Data: Born in Oklahoma City, Oklahoma, on April 1, 1969, the son of Jack and Maribeth Berry.

Education: Graduated from Wray High School, Wray, Colorado in May 1987; received Bachelor of Arts degree in Visual Arts from the University of Northern Colorado, Greeley, Colorado in December 1992. Completed the requirements for the Master of Science degree with a major in Geography at Oklahoma State University in May 1998.

Experience: Employed on farms in Yuma County, Colorado during summers in high school; employed as a house painter during summers at University of Northern Colorado; employed by Oklahoma State University, Department of Geography, as a graduate research assistant, 1993 to 1995.

Professional Memberships: Association of American Geographers, American Society of Photogrammetry and Remote Sensing.